Constrained Attitude Control of Uncertain Spacecraft with Appointed-Time Control Performance

Xuhui Lu, Yingmin Jia, Yongling Fu, Fumitoshi Matsuno

Constrained Attitude Control of Uncertain Spacecraft with Appointed-Time Control Performance

Xuhui Lu, Yingmin Jia, *Member, IEEE*, Yongling Fu, and Fumitoshi Matsuno, *Senior Member, IEEE*

***Abstract*—This paper studies the appointed-time attitude tracking control of the spacecraft on Special Orthogonal Group, with the attitude forbidden zone, the parameter uncertainties, and the external disturbances. A novel projection function is proposed, such that the normalized boresight vector of the sensitive instrument is mapped to a reduced dimensional vector in the Euclidean space. If the reduced dimensional vector is uniformly bounded, the constraint on the attitude forbidden zone will be satisfied at all the time. By virtue of the designed reduced dimensional vector and the associated auxiliary vectors, a set of vector-based error functions, the appointed-time performance constraints and the according switching law are carefully constructed. The proposed vector-based adaptive control scheme ensures that the spacecraft attitude can satisfy the attitude constraint and appointed-time control performance simultaneously, in the presence of parameter uncertainties and external disturbances. Simulation results show the effectiveness of the designed control scheme.**

***Index Terms*—Attitude tracking control, Prescribed performance control, Attitude constraint, Uncertainties.**

I. Introduction

The spacecraft attitude control has attracted much attention in recent years, due to its significance in many space missions [1]-[5]. However, it is still challenging to design the attitude control scheme of spacecraft. This is because the state space of the spacecraft attitude constitutes a nonlinear manifold named Special Orthogonal Group $SO(3)$ [6]-[9]. Besides, the spacecraft is inevitably subject to the parameter uncertainties and the external disturbances in the space environment [10]-[16]. The closed-loop stability of the spacecraft attitude control system will be deteriorated if the parameter uncertainties and the external disturbances are overlooked in the controller design. In face of the above problems, several breakthroughs have been made in the field of spacecraft attitude control [17]-[22]. In [23], a novel nonlinear terminal sliding mode attitude control input and the model predictive control method are combined to achieve the spacecraft attitude tracking, in the presence of the inertia uncertainties, the external disturbances and the actuator constraints. Several fault-tolerant attitude control schemes are also proposed in [24]-[28], to improve the robustness of the closed-loop system to the actuator faults.

Unfortunately, the above methods [17]-[28] are derived based upon the attitude parameterization of the rotation matrix on $SO(3)$, like the Euler angles, the quaternion and the modified Rodriguez parameters (MRPs). Notice that the Euler angles and the MRPs encounter singularity problem, and the quaternion-based continuous attitude control scheme suffers from the unwinding phenomenon. Hence, it is of great importance to design the attitude control scheme directly on $SO(3)$, to prevent the above problems. Sanyal et al. [29] design an attitude control scheme on $SO(3)$ to achieve almost global attitude tracking. In [30]-[31], the hybrid control method is successfully applied into the attitude control on $SO(3)$. In [32]-[33], the attitude synchronization control schemes are developed on $SO(3)$, for the general time-varying and directed communication graph. In [34], An adaptive passivity-based control scheme is also proposed to realize attitude tracking on $SO(3)$. In [35], a distributed observer is designed on $SO(3)$ to estimate the leader's state information, and the obtained $SO(3)$-based attitude consensus control scheme can avoid the measurement of the angular velocity.

However, notice that the methods in [17]-[35] do not consider the attitude constraints of the spacecraft. In fact, the boresight vectors of some sensitive instruments of the spacecraft should prevent direct exposure to the specific celestial objects. Therefore, to meet the according attitude constraints, several effective attitude trajectory planning schemes have been proposed [36]-[39]. Note that compared with the trajectory planning method [36]-[39], the potential-function-based attitude control method can ensure the closed-loop stability. In [40], the artificial potential function on the attitude constraints and the according constrained attitude stabilization control scheme are elaborately designed. In [41]-[42], the potential-function-based attitude stabilization control schemes are also developed and are robust to the external disturbances. A hierarchical controller is designed for the spacecraft attitude stabilization in [43], where the attitude constraints and the input saturation are both considered. Note that the methods in [40]-[43] are derived on the quaternion. Hence in [44], an adaptive constrained attitude control scheme is proposed on $SO(3)$, so that the robustness of the closed-loop system toward the external disturbances is enhanced. In [45], a velocity-free

Manuscript received ...

This work was supported by the NSFC (61327807,61521091, 61520106010, 61134005) and the National Basic Research Program of China (973 Program: 2012CB821200, 2012CB821201). *(Corresponding author: Yingmin Jia.)*

Xuhui Lu and Yongling Fu are with the School of Mechanical Engineering and Automation, Beihang University (BUAA), Beijing 100191, China (e-mails: luxuhui2018@163.com; fuyongling@buaa.edu.cn).

Yingmin Jia is with the Seventh Research Division and the Center for Information and Control, School of Automation Science and Electrical Engineering, Beihang University (BUAA), Beijing 100191, China (e-mails: ymjia@buaa.edu.cn).

Fumitoshi Matsuno is with the Department of Mechanical Engineering and Science, Kyoto University, Kyoto 606-8501, Japan (e-mail: matsuno@me.kyoto-u.ac.jp).

constrained attitude synchronization control scheme is also developed on $SO(3)$.

Besides, the results in [29]-[34] and [40]-[44] only ensure the closed-loop stability and the convergence of the attitude tracking/regulation error. However, the transient and steady control performance of the spacecraft attitude is essential to realize several space missions, and is challenging to be determined a priori [46]-[47]. Recently, the prescribed performance control method [48]-[50] has been proposed, where the prescribed performance control problem of the original control system is converted into the stabilization problem of an unconstrained nonlinear control system. Then several quaternion-based and MRPs-based prescribed performance attitude control schemes are designed [51]-[58]. In [59], a velocity-free prescribed-time attitude synchronization control scheme is derived on $SO(3)$. Zhou et al. [60] also put forward an $SO(3)$-based attitude tracking control scheme with the prescribed control performance, by virtue of a carefully-selected configuration error function. Unfortunately, note that the results in both [40]-[44] and [59]-[60] cannot satisfy the attitude constraint and achieve prescribed control performance simultaneously. The main difficulty to achieve the $SO(3)$-based constrained prescribed performance attitude tracking control is that $SO(3)$ is not a Euclidean space but a compact manifold without boundary. Additionally, it will become more complex to design the constrained attitude control scheme with prescribed control performance, if the spacecraft is subject to the parameter uncertainties and the external disturbances.

Motivated by above discussion and analysis, this paper aims to study the attitude tracking control of the spacecraft on $SO(3)$ with appointed-time control performance, in the presence of the attitude constraint, the parameter uncertainties and the external disturbances. To meet the attitude constraint and the appointed-time control performance simultaneously, a novel projection function is carefully constructed, such that the boresight vector of the sensitive instrument is mapped to a reduced dimensional vector in the Euclidean space $\mathbb{R}^2$. If the obtained reduced dimensional vector is uniformly bounded, the spacecraft attitude will keep away from the attitude forbidden zone. Then, based upon the reduced dimensional vector, the according auxiliary vectors are also constructed. Correspondingly, a set of vector-based error functions, the appointed-time performance constraints and the vector-based switched controller are carefully designed. Compared with the control schemes in [40]-[44] and [59]-[60], by means of the designed attitude control scheme, the spacecraft attitude on $SO(3)$ can meet the attitude constraint and the appointed-time control performance simultaneously. Moreover, to attenuate the effects of the parameter uncertainties and the external disturbances, two dynamic gaining variables are designed and introduced into the control input. Compared with the control schemes in [44] and [59], by virtue of the designed dynamic gaining variables, the proposed adaptive control scheme can be robust toward the parameter uncertainties and the external disturbances, without the need to estimate the uncertain parameters.

The rest of this paper is organized as follows. Section II is the preliminaries, including the notations, the attitude motion modeling of the spacecraft, the description of the attitude constraint, the introduction of the appointed-time performance function and the error transformation, and the problem formulation. Section III is the controller design. Section IV is the simulation results. The conclusions are drawn in Section V.

II. Preliminaries

A. Notations

First, $\mathbb{R}^n$ and $\mathbb{R}^{m\times n}$ are the real n-dimensional vector space and the real $(m\times n)$-dimensional matrix space respectively. $0_n \in \mathbb{R}^n$ is the zero vector, and $E_n \in \mathbb{R}^{n\times n}$ is the identity matrix. $\|z\|$ is the 2-norm of the vector $z\in\mathbb{R}^n$. $\|B\|$, $\mathrm{rank}(B)$, $\mathrm{Tr}(B)$ are the 2-norm, the rank and the trace of the matrix $B\in\mathbb{R}^{n\times n}$ respectively. For any matrix $B\in\mathbb{R}^{m\times n}$ with $m\le n$, $B^\dagger$ is the pseudo-inverse of the matrix B, and $B^\dagger = B^T(BB^T)^{-1}$ if B is full row rank. For any vector $b=\mathrm{col}(b_1,b_2,b_3)\in\mathbb{R}^3$, the function $S(\cdot)$ is defined as $S(b)=[0,-b_3,b_2;b_3,0,-b_1;-b_2,b_1,0]$, and the function $\mathrm{Pa}(\cdot)$ is defined as $\mathrm{Pa}(S(b))=b$. For any vector $z=[z_i]_n\in\mathbb{R}^n$, $\tanh(z)\triangleq\mathrm{col}(\tanh(z_1),\ldots,\tanh(z_n))$ is the hyperbolic tangent function with $\tanh(z_i)=\frac{\exp(z_i)-\exp(-z_i)}{\exp(z_i)+\exp(-z_i)}$.

Moreover, the Special Orthogonal Group $SO(3)$ is used to describe the spacecraft attitude and is defined as [29]-[32]

$$SO(3)\triangleq\{\bar{Q}\in\mathbb{R}^{3\times3}\mid \bar{Q}^T\bar{Q}=E_3,\det(\bar{Q})=1\}. \quad (1)$$

Based on the Rodrigues′ formula, the rotation matrix $\bar{Q}\in SO(3)$ can be represented as [60]

$$\bar{Q}=E_3+\frac{\sin(\|\phi_Q\|)}{\|\phi_Q\|}S(\phi_Q)+\frac{1-\cos(\|\phi_Q\|)}{\|\phi_Q\|^2}S^2(\phi_Q), \quad (2)$$

where the vector $\phi_Q\in\mathbb{R}^3$ satisfies $\|\phi_Q\|\le\pi$.

B. Attitude Motion Modeling of the Spacecraft

First, the inertia frame and the body-attached frame of the spacecraft are denoted by $\mathcal{F}_i$ and $\mathcal{F}_b$ respectively. The attitude kinematics and dynamics of the spacecraft are [29]-[32]

$$\dot{Q}=QS(w), \quad (3a)$$

$$J\dot{w}=-S(w)Jw+\tau+d, \quad (3b)$$

where $Q\in SO(3)$ is the spacecraft attitude representing the rotation from $\mathcal{F}_i$ to $\mathcal{F}_b$ expressed in $\mathcal{F}_b$, $w\in\mathbb{R}^3$ is the angular velocity of the spacecraft in $\mathcal{F}_b$, $\tau\in\mathbb{R}^3$ is the control input, $d(t)\in\mathbb{R}^3$ are the time-varying and bounded external disturbances, $J\in\mathbb{R}^{3\times3}$ is the inertia matrix, and the matrix $S(w)\in\mathbb{R}^{3\times3}$ is defined in Notations. Besides, the following property holds for the spacecraft [24]-[27].

Property 1: J is positive definite and is bounded, that is, there exist two positive constants $\lambda_{J,max}$ and $\lambda_{J,min}$ such that $\lambda_{J,min}E_3<J<\lambda_{J,max}E_3$. Besides, the disturbances $d(t)$ are uniformly bounded, meaning that there exists a constant $\Delta_d>0$ so that $\|d(t)\|<\Delta_d$ at all the time. ■

C. Attitude forbidden zone of the spacecraft

Here the spacecraft should satisfy the attitude constraint. To be specific, $v_{b,1} \in \mathbb{R}^3$ denotes the normalized boresight vector of the sensitive instrument in $\mathcal{F}_b$, and $v_{r,1} \triangleq Qv_{b,1} \in \mathbb{R}^3$ is the according normalized boresight vector in $\mathcal{F}_i$. Here the vector $v_{b,1}$ is constant. Besides, $v_f \in \mathbb{R}^3$ denotes a normalized vector in $\mathcal{F}_i$, which stands for the orientation toward the undesired space object. For the spacecraft, the angle between $v_{r,1}$ and v_f should be larger than $\theta_f \in [0, \pi)$ which is the minimum allowable angle between these two vectors. Correspondingly, the constraint on the attitude forbidden zone can be formulated as [39]

$$v_f^T v_{r,1} < \cos\theta_f. \tag{4}$$

Then denote

$$\eta \triangleq \cos\theta_f - v_f^T v_{r,1}. \tag{5}$$

Note that the constraint (4) holds if and only if $\eta(t) > 0$.

D. Appointed-time performance function and error transformation

Here consider a general non-negative error function $y(t) \geq 0$. $y(t)$ will possess the prescribed control performance, if it satisfies the following constraint at all the time

$$y(t) < \rho_y(t), \tag{6}$$

where $\rho_y(t) = \rho(\rho_0, \rho_\infty, t_0, t_f, t)$ is the according appointed-time decaying function and is defined as

$$\rho(\rho_0, \rho_\infty, t_0, t_f, t) \triangleq \begin{cases} \frac{\rho_0 - \rho_\infty}{t_f^2}(t_0 + t_f - t)^2 + \rho_\infty, & t_0 \leq t < t_0 + t_f; \\ \rho_\infty, & t \geq t_0 + t_f, \end{cases} \tag{7}$$

with the parameters ρ_0, ρ_∞, t_0 and t_f satisfying $\rho_0 > \rho_\infty > 0$ and $t_f > t_0 \geq 0$. Besides, it is obtained from (6)-(7) that

$$\dot{\rho}(\rho_0, \rho_\infty, t_0, t_f, t) = \begin{cases} -\frac{2(\rho_0 - \rho_\infty)}{t_f^2}(t_0 + t_f - t), & t_0 \leq t < t_0 + t_f; \\ 0, & t \geq t_0 + t_f. \end{cases} \tag{8}$$

Remark 1: The meanings and the effects of the parameters in the appointed-time decaying function $\rho_y(t)$ are discussed here [48]-[58]. First, the parameters t_0 is the activation time of the constraint (6), meaning that from the time t_0, the variable $y(t)$ should meet the constraint (6) (that is, $y(t_0) < \rho_y(t_0)$). The parameter ρ_0 is the initial value of the decaying function $\rho_y(t)$, that is, $\rho_y(t_0) = \rho_0$. The parameters ρ_∞ and t_f are the steady value and the setting time interval of the decaying function $\rho_y(t)$ respectively, that is, $\rho_y(t) \equiv \rho_\infty$ when $t \geq t_0 + t_f$. Notice that if the constraint (6) holds for any $t \geq t_0$, the function $y(t)$ will fall into the interval $[0, \rho_\infty)$ with the setting time interval t_f s, meaning that $\sup_{t \geq t_0 + t_f} y(t) \leq \rho_\infty$.

In addition, since $\rho_\infty < \rho_0$, it is obtained from (7)-(8) that $\frac{d\rho_y(t)}{dt} < 0$ when $t_0 \leq t < t_0 + t_f$. Therefore the function $\rho_y(t)$ monotonically decreases from ρ_0 to ρ_∞ in the time interval $[t_0, t_0 + t_f]$, and remains at ρ_∞ when $t \geq t_0 + t_f$. It can be also seen in (7) that $\rho_y(t) \geq \rho_\infty > 0$ for any $t \geq t_0$. ■

According to the constraint (6), the following prescribed performance error function is designed

$$W_e(y_\rho) \triangleq -\ln(1 - y_\rho), \tag{9}$$

where $y_\rho(t) \triangleq \frac{y(t)}{\rho_y(t)}$, and $y_\rho(t) \geq 0$ since $y(t) \geq 0$ and $\rho_y(t) > 0$. Note that $W_e = 0$ if and only if $y_\rho = 0$, meaning that $W_e = 0$ if and only if $y = 0$. Besides, W_e will tend to positive infinity if y_ρ tends to 1, and W_e will be finite if $y_\rho < 1$. Moreover, it is obtained from (9) that

$$\frac{dW_e}{dt} = \Phi(y_\rho)(\frac{1}{\rho_y}\dot{y} - \frac{\dot{\rho}_y}{\rho_y^2}y), \tag{10}$$

if $0 \leq y_\rho < 1$, where

$$\Phi(y_\rho) \triangleq \frac{\partial W_e}{\partial y_\rho} = \frac{1}{1 - y_\rho}. \tag{11}$$

Note that $\Phi(y_\rho) \geq 1$ and

$$W_e(y_\rho) \leq \Phi(y_\rho)y_\rho \leq \Phi^2(y_\rho)y_\rho, \tag{12}$$

if $0 \leq y_\rho < 1$ (that is, the constraint (6) is satisfied).

E. Problem formulation

In this paper, the spacecraft is controlled to achieve attitude tracking. The reference attitude, the reference angular velocity, and the reference angular acceleration are denoted by $Q_d(t) \in SO(3)$, $w_d(t) \in \mathbb{R}^3$ and $a_d(t) \in \mathbb{R}^3$ respectively, and $\mathcal{F}_{b,d}$ denotes the body-attached frame of the desired spacecraft attitude Q_d. The reference attitude $Q_d(t)$ and the reference angular velocity $w_d(t)$ obey the following equation

$$\dot{Q}_d = Q_d S(w_d). \tag{13}$$

Notice that the desired attitude $Q_d(t)$ represents the rotation from $\mathcal{F}_i$ to $\mathcal{F}_{b,d}$ expressed in $\mathcal{F}_{b,d}$, and $w_d(t)$ is the desired angular velocity in $\mathcal{F}_{b,d}$. Here the desired attitude $Q_d(t)$ meets the constraint (4) at all the time, and $w_d(t)$ and $a_d(t)$ are both uniformly bounded. This means that there exist two constants $\Delta_w > 0$ and $\Delta_a > 0$ such that $\|w_d(t)\| < \Delta_w$ and $\|a_d(t)\| < \Delta_a$. Besides, denote $v_{r,d,1} \triangleq Q_d v_{b,1}$, $Q_{er} \triangleq Q_d^T Q$, $\bar{w}_d \triangleq Q_{er}^T w_d$, and $w_{er} \triangleq w - \bar{w}_d$. It is obtained from (3a)-(3b) and (13) that

$$\dot{Q}_{er} = Q_{er} S(w_{er}), \tag{14a}$$

$$\begin{aligned} J\dot{w}_{er} = &- S(\bar{w}_d)J\bar{w}_d - JQ_{er}^T a_d + S(Jw)w_{er} \\ &- (S(\bar{w}_d)J + JS(\bar{w}_d))w_{er} + \tau + d. \end{aligned} \tag{14b}$$

Then the problem to be studied is provided as follows.

Problem 1: For the spacecraft with the parameter uncertainties and the external disturbances, a control scheme should be designed, so that the spacecraft attitude $Q(t)$ can track the trajectory $Q_d(t)$ with the appointed-time control performance, and the attitude constraint (4) can be satisfied at all the time.

Besides, the following lemma will be used later.

Lemma 1: For a positive semidefinite matrix $P \in \mathbb{R}^{3\times3}$ with $\mathrm{rank}(P) \geq 2$, its eigenvalues are $\lambda_{P,i}$, $i = 1, 2, 3$, with $\lambda_{P,1} \geq \lambda_{P,2} \geq \lambda_{P,3} \geq 0$. Then it follows that $\mathrm{Tr}(P - P\bar{Q}) \geq \frac{\lambda_{P,2} + \lambda_{P,3}}{2}\mathrm{Tr}(E_3 - E_3\bar{Q})$ for any rotation matrix $\bar{Q} \in SO(3)$. ■

The proof of Lemma 1 can be seen in [61].

III. Constrained appointed-time attitude controller design

In this section, a control scheme will be designed to realize constrained attitude tracking. First, $v_{b,2} \in \mathbb{R}^3$ and $v_{b,3} \in \mathbb{R}^3$ denote two unit vectors in $\mathcal{F}_b$, so that $v_{b,i}$, $i = 1, 2, 3$, are perpendicular to each other, and $v_{b,3} = S(v_{b,1})v_{b,2}$. It means that $v_{b,i}^T v_{b,j} = 0$ for any $i = 1, 2, 3$ and $j = 1, 2, 3$ with $i \neq j$. Denote $v_{r,2} \triangleq Qv_{b,2}$, $v_{r,d,2} \triangleq Q_d v_{b,2}$, $v_{r,3} \triangleq Qv_{b,3}$, $v_{r,d,3} \triangleq Q_d v_{b,3}$, $U_b \triangleq [v_{b,1}, v_{b,2}, v_{b,3}]$, $U_r \triangleq [v_{r,1}, v_{r,2}, v_{r,3}]$ and $U_{r,d} \triangleq [v_{r,d,1}, v_{r,d,2}, v_{r,d,3}]$. Note that $v_{r,3} = S(v_{r,1})v_{r,2}$, $v_{r,d,3} = S(v_{r,d,1})v_{r,d,2}$, $\|v_{r,i}\| = \|v_{r,d,i}\| = 1$ for any $i = 1, 2, 3$, $U_b^T U_b = U_r^T U_r = U_{r,d}^T U_{r,d} = E_3$, $Q = U_r U_b^T$, and $Q_d = U_{r,d} U_b^T$. Besides, if $v_{r,1} = v_{r,d,1}$ and $v_{r,2} = v_{r,d,2}$, it is obtained that $v_{r,3} = v_{r,d,3}$ and accordingly $Q = Q_d$. This means that if the vectors $v_{r,1}$ and $v_{r,2}$ converge to $v_{r,d,1}$ and $v_{r,d,2}$ respectively, the attitude Q will converge to Q_d. In addition, based upon (3a) and (13), the derivatives of $v_{r,i}$ and $v_{r,d,i}$ are

$$\dot{v}_{r,i} = QS(w)v_{b,i} = -S(v_{r,i})Qw, \tag{15a}$$

$$\dot{v}_{r,d,i} = Q_d S(w_d)v_{b,i} = -S(v_{r,d,i})Q_d w_d. \tag{15b}$$

A. The projection function on the attitude constraint

In this paper, the spacecraft attitude should meet the constraint (4) at all the time, and besides the attitude tracking error should possess the appointed-time control performance. However, the state space of the spacecraft attitude, that is, $SO(3)$, is not an Euclidean space like $\mathbb{R}^3$, which complicates the control scheme design to meet the constraint (4) and the appointed-time control performance simultaneously. Hence, a novel reduced dimensional vector $x \in \mathbb{R}^2$ is designed as

$$x \triangleq \Pr(v_{r,1}), \tag{16}$$

where

$$\Pr(v_{r,1}) \triangleq \frac{\cos\theta_f + 1}{\eta} N_f v_{r,1}, \tag{17}$$

is the according projection function, η is defined in (5), and the matrix $N_f \triangleq [v_{p,1}^T; v_{p,2}^T] \in \mathbb{R}^{2\times 3}$ satisfies $\|v_{p,1}\| = \|v_{p,2}\| = 1$, $v_{p,1}^T v_{p,2} = 0$ and $S(v_{p,1})v_{p,2} = v_f$. It is obtained from the definition of N_f that $N_f N_f^T = E_2$ and $N_f v_f = 0_2$.

Similarly, we can also obtain the reduced dimensional vector associated with $v_{r,d,1}$, that is,

$$x_d \triangleq \Pr(v_{r,d,1}) \in \mathbb{R}^2. \tag{18}$$

In addition, for the vectors $v_{r,1}$ and $v_{r,d,1}$, and the reduced dimensional vectors x and x_d, the following lemmas hold.

Lemma 2: For the vectors $v_{r,1}$ and x, if $v_{r,1}$ satisfies the constraint (4), x will be bounded. ■

The proof of Lemma 2 can be seen in [61].

Lemma 3: For $v_{r,1}(t)$ and $x(t)$, if $v_{r,1}(0)$ satisfies the constraint (4) and $x(t)$ is uniformly bounded in $[0, \acute{t})$, where $0 < \acute{t} \leq +\infty$, then the constraint (4) always holds in $[0, \acute{t})$. ■

The proof of Lemma 3 can be seen in [61].

Lemma 4: If both $v_{r,1}$ and $v_{r,d,1}$ satisfy the constraint (4), then $\|v_{r,1} - v_{r,d,1}\| \leq \|x - x_d\|$ will hold. Moreover, $\|v_{r,1} - v_{r,d,1}\| = \|x - x_d\|$ if and only if $v_{r,1} = v_{r,d,1}$. ■

The proof of Lemma 4 can be seen in [61].

Note that $Q_d(t)$ satisfies the constraint (4) at all the time, and therefore it follows from Lemma 2 that $x_d(t)$ is uniformly bounded at all the time. Moreover, in view of (15a) and (16)-(17), the derivative of x is

$$\dot{x} = -\frac{1}{\eta^2} Gw, \tag{19}$$

where

$$G \triangleq (\cos\theta_f + 1)N_f(\eta E_3 + v_{r,1}v_f^T)S(v_{r,1})Q. \tag{20}$$

Accordingly, the following lemma holds for $G \in \mathbb{R}^{2\times 3}$.

Lemma 5: The matrix G is bounded. Besides, if the constraint (4) is satisfied, the matrix GG^T will be positive definite. This means that there exist two positive constants $\lambda_{G,min}$ and $\lambda_{G,max}$ such that $\lambda_{G,min} E_2 \leq GG^T \leq \lambda_{G,max} E_2$. ■

The proof of Lemma 5 can be seen in [61].

Similarly, it is obtained from (15b) and (17)-(18) that

$$\dot{x}_d = -\frac{1}{\eta_d^2} G_d w_d, \tag{21}$$

where $\eta_d \triangleq \cos\theta_f - v_f^T v_{r,d,1}$ and $G_d \triangleq (\cos\theta_f + 1)N_f(\eta_d E_3 + v_{r,d,1}v_f^T)S(v_{r,d,1})Q_d$. Based upon Lemma 5, it follows that the matrix $G_d(t)$ is uniformly bounded, and since $\eta_d(t) > 0$ at all the time and $w_d(t)$ is uniformly bounded, it is further obtained that $\dot{x}_d(t)$ is also uniformly bounded.

Remark 2: It should be noted that based upon the projection function (17), the unit vectors $v_{r,1}(t)$ and $v_{r,d,1}(t)$ are mapped to the reduced dimensional vectors $x(t)$ and $x_d(t)$ in the Euclidean space $\mathbb{R}^2$ respectively. Note that if $x(t)$ is uniformly bounded and the initial attitude $Q(0)$ meets the constraint (4), it is ensured in Lemma 3 that the attitude constraint (4) is satisfied at all the time. Besides, since $x_d(t)$ is uniformly bounded, it further follows that in order to satisfy the constraint (4) at all the time, the control scheme is only required to ensure the uniformly boundedness of $\|x(t) - x_d(t)\|$, if $v_{r,1}(0)$ meets the constraint (4). ■

B. Vector-based error functions and appointed-time performance constraints

First, denote

$$x_{er} \triangleq x - x_d, \tag{22}$$

as the tracking error with respect to x_d. Then the following auxiliary vectors are introduced

$$\bar{v}_{r,d,2} \triangleq \frac{\tilde{v}_{r,d,2}}{\|\tilde{v}_{r,d,2}\|}, \tag{23a}$$

$$\bar{v}_{r,d,3} \triangleq \frac{\tilde{v}_{r,d,3}}{\|\tilde{v}_{r,d,3}\|}, \tag{23b}$$

where

$$\tilde{v}_{r,d,2} \triangleq S(v_{r,1})v_{r,d,2}, \tag{24a}$$

$$\tilde{v}_{r,d,3} \triangleq (E_3 - v_{r,1}v_{r,1}^T)v_{r,d,2}. \tag{24b}$$

Based upon (23a)-(23b) and (24a)-(24b), it is further obtained that $v_{r,1}^T \tilde{v}_{r,d,2} = v_{r,1}^T \bar{v}_{r,d,2} = v_{r,1}^T \tilde{v}_{r,d,3} = v_{r,1}^T \bar{v}_{r,d,3} = \tilde{v}_{r,d,2}^T \tilde{v}_{r,d,3} = \bar{v}_{r,d,2}^T \bar{v}_{r,d,3} = 0$. Since $v_{r,1}^T \bar{v}_{r,d,2} = v_{r,1}^T \bar{v}_{r,d,3} =$

0, $S(v_{r,2})v_{r,1} = -v_{r,3}$ and $\sum_{i=1}^{3}(\acute{z}^T v_{r,i})^2 = 1$ for any unit vector $\acute{z} \in \mathbb{R}^3$, it is obtained that

$$\begin{aligned}(\bar{v}_{r,d,2}^T S(v_{r,2})v_{r,1})^2 &= (\bar{v}_{r,d,2}^T v_{r,3})^2 + (v_{r,1}^T \bar{v}_{r,d,2})^2 \\ &= 1 - (\bar{v}_{r,d,2}^T v_{r,2})^2,\end{aligned} \tag{25a}$$

$$\begin{aligned}(\bar{v}_{r,d,3}^T S(v_{r,2})v_{r,1})^2 &= (\bar{v}_{r,d,3}^T v_{r,3})^2 + (v_{r,1}^T \bar{v}_{r,d,3})^2 \\ &= 1 - (\bar{v}_{r,d,3}^T v_{r,2})^2.\end{aligned} \tag{25b}$$

In view of (15a)-(15b) and (23a)-(23b), the derivatives of $\bar{v}_{b,d,2}$ and $\bar{v}_{b,d,3}$ are

$$\begin{aligned}\dot{\bar{v}}_{r,d,2} =& \frac{1}{\|\tilde{v}_{r,d,2}\|}\Psi_2(-S(v_{r,1})S(v_{r,d,2})Q_d w_d \\ &+ S(v_{r,d,2})S(v_{r,1})Qw),\end{aligned} \tag{26a}$$

$$\begin{aligned}\dot{\bar{v}}_{r,d,3} =& \frac{1}{\|\tilde{v}_{r,d,3}\|}\Psi_3(-(E_3 - v_{r,1}v_{r,1}^T)S(v_{r,d,2})Q_d w_d \\ &+ \Psi_4 Qw).\end{aligned} \tag{26b}$$

where $\Psi_2 \triangleq E_3 - \bar{v}_{r,d,2}\bar{v}_{r,d,2}^T$, $\Psi_3 \triangleq E_3 - \bar{v}_{r,d,3}\bar{v}_{r,d,3}^T$ and $\Psi_4 \triangleq (v_{r,1}^T v_{r,d,2}E_3 + v_{r,1}v_{r,d,2}^T)S(v_{r,1})$.

Then, the following vector-based error functions are constructed

$$\varphi_1 \triangleq \frac{1}{2}\|x_{er}\|^2, \tag{27a}$$

$$\varphi_2 \triangleq 1 - \bar{v}_{r,d,2}^T v_{r,2}, \tag{27b}$$

$$\varphi_3 \triangleq 1 - \bar{v}_{r,d,3}^T v_{r,2}. \tag{27c}$$

On one hand, the appointed-time performance constraint on φ_1 is designed as

$$\varphi_1(t) < \rho_1(t), \tag{28}$$

where $\rho_1(t) \triangleq \rho(\rho_{0,1}, \rho_{\infty,1}, 0, t_{f,1}, t)$ with $0 < \rho_{\infty,1} < \min\{\rho_{0,1}, 1\}$ and $t_{f,1} > 0$. Here the parameter $\rho_{0,1}$ is designed such that the constraint (28) holds at the initial instant.

On the other hand, two time instants t_s and $\bar{t}_f$ are designed as

$$t_c \triangleq \begin{cases} t_{f,1}, & \varphi_3(t_{f,1}) \le 2 - \epsilon_1; \\ t_{f,1} + t_{f,2}, & \varphi_3(t_{f,1}) > 2 - \epsilon_1, \end{cases} \tag{29a}$$

$$\bar{t}_f \triangleq t_c + t_{f,3}, \tag{29b}$$

where $0 < \epsilon_1 < 1$, $t_{f,2} > 0$ and $t_{f,3} > 0$. It can be seen in (29a)-(29b) that $t_c = t_{f,1}$ and $\bar{t}_f = t_{f,1} + t_{f,3}$ when $\varphi_3(t_{f,1}) \le 2 - \epsilon_1$, and $t_c = t_{f,1} + t_{f,2}$ and $\bar{t}_f = t_{f,1} + t_{f,2} + t_{f,3}$ when $\varphi_3(t_{f,1}) > 2 - \epsilon_1$. In view of (29a), if $\varphi_3(t_{f,1}) > 2 - \epsilon_1$ and accordingly $t_c = t_{f,1} + t_{f,2}$, the following appointed-time performance constraint on φ_2 is constructed in the time interval $t \in [t_{f,1}, t_{f,1} + t_{f,2})$

$$\varphi_2(t) < \rho_2(t), \tag{30}$$

where $\rho_2(t) = \rho(\rho_{0,2}, \rho_{\infty,2}, t_{f,1}, t_{f,2}, t)$ with $0 < \rho_{\infty,2} < 1 - \sqrt{1 - (1 - \epsilon_1)^2}$ and $1 + \sqrt{1 - (1 - \epsilon_1)^2} \le \rho_{0,2} < 2$. Then, when $t \ge t_c$, the following appointed-time performance constraint on φ_3 is constructed in the time interval $[t_c, +\infty)$

$$\varphi_3(t) < \rho_3(t), \tag{31}$$

where $\rho_3(t) = \rho(\rho_{0,3}, \rho_{\infty,3}, t_c, t_{f,3}, t)$, with $0 < \rho_{\infty,3} < 1$ and $2 - \epsilon_1 < \rho_{0,3} < 2$.

In addition, the following lemma holds for $\varphi_1(t)$ and $\varphi_3(t)$.

Lemma 6: If $\varphi_1 < \rho_{\infty,1}$ and $\varphi_3 < \rho_{\infty,3}$, the attitude tracking error Q_{er} will be in the set

$$\Theta_R \triangleq \{Q_{er} \in SO(3) \mid \mathrm{Tr}(E_3 - Q_{er}) < 4\rho_{\infty,1} + 2\rho_{\infty,3}\}, \tag{32}$$

which is a small neighborhood of the equilibrium E_3. ■

The proof of Lemma 6 can be seen in Appendix A.

Remark 3: Here the choice of the parameter $\rho_{\infty,1}$ is discussed as follows. On one hand, if $\rho_{\infty,1} < \rho_{0,1}$, it follows from (8) that $\dot{\rho}_1(t) < 0$ when $t \in [0, t_{f,1})$, and $\dot{\rho}_1(t) = 0$ when $t \ge t_{f,1}$. This means that the parameter $\rho_{\infty,1}$ should be selected as $\rho_{\infty,1} < \rho_{0,1}$, so that the function $\rho_1(t)$ is strictly monotonically decreasing in the time interval $[0, t_{f,1})$, and remains its value when $t \ge t_{f,1}$ (that is, $\rho_1(t) = \rho_{\infty,1}$ when $t \ge t_{f,1}$).

On the other hand, if $\varphi_1(t)$ meets the constraint (28), it follows from Lemma 4 that $1 - v_{r,d,1}^T(t)v_{r,1}(t) < \rho_1(t)$. Especially, if $\varphi_1(t) < \rho_{\infty,1}$, it also follows from Lemma 4 that

$$1 - v_{r,d,1}^T(t)v_{r,1}(t) = \frac{1}{2}\|v_{r,1}(t) - v_{r,d,1}(t)\|^2 < \rho_{\infty,1}. \tag{33}$$

Accordingly, if the parameter $\rho_{\infty,1}$ is set as $\rho_{\infty,1} < 1$, it can be obtained from (33) that

$$v_{r,d,1}^T(t)v_{r,1}(t) > 1 - \rho_{\infty,1} > 0. \tag{34}$$

Besides, according to (24a)-(24b), it is obtained that

$$\|\tilde{v}_{r,d,2}(t)\|^2 = \|\tilde{v}_{r,d,3}(t)\|^2 = 1 - (v_{r,1}^T(t)v_{r,d,2}(t))^2. \tag{35}$$

Notice that $\acute{z}^T U_{r,d} U_{r,d}^T \acute{z} = \sum_{i=1}^{3}(v_{r,d,i}^T \acute{z})^2 = 1$ for any unit vector $\acute{z} \in \mathbb{R}^3$. Accordingly, from (34)-(35), it follows that

$$\begin{aligned}\|\tilde{v}_{r,d,2}(t)\|^2 =& \|\tilde{v}_{r,d,3}(t)\|^2 \\ =& (v_{r,1}^T(t)v_{r,d,1}(t))^2 + (v_{r,1}^T(t)v_{r,d,3}(t))^2 \\ \ge& (v_{r,1}^T(t)v_{r,d,1}(t))^2 \\ >& (1 - \rho_{\infty,1})^2 \\ >& 0,\end{aligned} \tag{36}$$

if $\rho_{\infty,1} < 1$. Since $\|\tilde{v}_{r,d,2}(t)\| = \|\tilde{v}_{r,d,3}(t)\| > (1 - \rho_{\infty,1}) > 0$ when $\rho_{\infty,1} < 1$, the vectors $\bar{v}_{r,d,2}(t)$ (23a) and $\bar{v}_{r,d,3}(t)$ (23b) can be obtained. This means that the parameter $\rho_{\infty,1}$ should be selected as $\rho_{\infty,1} < 1$, in order to obtain the vectors $\bar{v}_{r,d,2}(t)$ (23a) and $\bar{v}_{r,d,3}(t)$ (23b) when $\varphi_1(t) < \rho_{\infty,1}$. Based upon the above analysis, it is obtained that the parameter $\rho_{\infty,1}$ should be chosen as $\rho_{\infty,1} < \min\{\rho_{0,1}, 1\}$. ■

Remark 4: It should be noticed that if the constraint (28) holds at all the time, it is obtained from Remark 2 that the attitude constraint (4) is satisfied at all the time. Besides, if the constraint (28) holds at all the time, it follows that that Eq. (33) holds when $t \ge t_{f,1}$. From (33), it further follows that

$$\|v_{r,1}(t) - v_{r,d,1}(t)\| < \sqrt{2\rho_{\infty,1}}, \tag{37}$$

when $t \ge t_{f,1}$. It can be seen in (37) that the smaller the parameter $\rho_{\infty,1}$ is, the smaller the error between the vectors $v_{r,1}(t)$ and $v_{r,d,1}(t)$ becomes when $t \ge t_{f,1}$. ■

Remark 5: Here, the choice of the range of the parameters $\rho_{0,2}$, $\rho_{\infty,2}$, $\rho_{0,3}$ and $\rho_{\infty,3}$ is discussed as below. First, when $\varphi_3(t_{f,1}) \le 2 - \epsilon_1$, it follows from (29a) and (31) that $t_c =$

$t_{f,1}$ and accordingly the error function $\varphi_3(t)$ should obey the constraint (31) for any $t \geq t_{f,1}$. Hence, the parameter $\rho_{0,3}$ is set as $\rho_{0,3} > 2-\epsilon_1$, meaning that $\varphi_3(t_{f,1}) \leq 2-\epsilon_1 < \rho_{0,3}$ and the constraint (31) is satisfied when $t = t_{f,1}$. The parameter $\rho_{\infty,3}$ is then set as $0 < \rho_{\infty,3} < 1$ such that $\rho_{\infty,3} < 1 < 2-\epsilon_1 < \rho_{0,3}$, meaning that the requirement on the monotonic decrease of the function $\rho_3(t)$ can be satisfied.

Besides, when $\varphi_3(t_{f,1}) = 1 - \bar{v}_{r,d,3}^T(t_{f,1})v_{r,2}(t_{f,1}) > 2-\epsilon_1$, it follows from (29a) that $t_c = t_{f,1} + t_{f,2}$. Since the parameter $\rho_{0,2}$ is set as $1+\sqrt{1-(1-\epsilon_1)^2} \leq \rho_{0,2} < 2$, it follows from $v_{r,1}^T\bar{v}_{r,d,2} = v_{r,1}^T\bar{v}_{r,d,3} = \bar{v}_{r,d,2}^T\bar{v}_{r,d,3} = v_{r,1}^Tv_{r,2} = 0$ and $\bar{v}_{r,d,3}^T(t_{f,1})v_{r,2}(t_{f,1}) < -1+\epsilon_1$ that $\varphi_2(t_{f,1}) \leq 1+\sqrt{(\bar{v}_{r,d,2}^T(t_{f,1})v_{r,2}(t_{f,1}))^2} = 1+\sqrt{1-(\bar{v}_{r,d,3}^T(t_{f,1})v_{r,2}(t_{f,1}))^2} < 1+\sqrt{1-(1-\epsilon_1)^2} \leq \rho_{0,2}$, meaning that the constraint (30) is satisfied when $t = t_{f,1}$. In addition, since the parameter $\rho_{\infty,2}$ is set as $\rho_{\infty,2} < 1-\sqrt{1-(1-\epsilon_1)^2}$, if $\varphi_2(t_c) = 1-\bar{v}_{r,d,2}^T(t_c)v_{r,2}(t_c) < \rho_{\infty,2}$, it is similarly obtained from $v_{r,1}^T\bar{v}_{r,d,2} = v_{r,1}^T\bar{v}_{r,d,3} = \bar{v}_{r,d,2}^T\bar{v}_{r,d,3} = v_{r,1}^Tv_{r,2} = 0$ that $\varphi_3(t_c) \leq 1+\sqrt{(\bar{v}_{r,d,3}^T(t_c)v_{r,2}(t_c))^2} = 1+\sqrt{1-(\bar{v}_{r,d,2}^T(t_c)v_{r,2}(t_c))^2} < 2-\epsilon_1 < \rho_{0,3}$. This means that if the constraint (30) is satisfied when $t = t_c$, the according constraint (31) will also hold when $t = t_c$.

In all, the range of the parameter $\rho_{0,2}$ is set to ensure that the constraint (30) holds when $t = t_{f,1}$ and $\varphi_3(t_{f,1}) > 2-\epsilon_1$, the ranges of the parameters $\rho_{0,3}$ and $\rho_{\infty,2}$ are set to guarantee that the constraint (31) holds when $t = t_c$, and the range of the parameter $\rho_{\infty,3}$ is set to ensure that the function $\rho_3(t)$ is monotonically decreasing. ■

Remark 6: If the constraint (28) holds at all the time, and the constraint (31) always holds when $t \geq t_c$, it follows that $\varphi_1(t) < \rho_{\infty,1}$ and $\varphi_3(t) < \rho_{\infty,3}$ when $t \geq \bar{t}_f$. Hence, to realize the desired control performance, the control scheme should be designed so that the constraint (28) holds at all the time, and the constraint (31) always holds when $t \geq t_c$.

Besides, based on Remark 1, if the parameters $\rho_{\infty,i}$, $i = 1,2,3$, get larger (smaller), the steady values of the functions $\rho_i(t)$, $i = 1,2,3$, will be larger (smaller), the size of the residual set Θ_R (32) will be larger (smaller), and the steady-state error of the tracking error $R_{er}(t)$ will also be larger (smaller). In addition, based on Remark 1, if the parameters $t_{f,i}$, $i = 1,2,3$, get larger (smaller), the setting time intervals of the functions $\rho_i(t)$, $i = 1,2,3$, will be larger (smaller), and the setting time $\bar{t}_f$ (29b) of the tracking error $R_{er}(t)$ will also be larger (smaller). ■

C. Virtual controller design

First, based upon the error functions (27a)-(27c), and the appointed-time performance constraints (28) and (30)-(31), the virtual attitude controller is designed as

$$w_c = w_{c,1} + \lambda_c v_{b,1}, \tag{38}$$

where

$$w_{c,1} \triangleq \frac{k_{c,1}}{\eta^2}G^\dagger\Phi_1 x_{er}, \tag{39a}$$

$$\lambda_c \triangleq \begin{cases} 0, & 0 \leq t < t_{f,1}; \\ -k_{c,2}\Phi_2\bar{v}_{r,d,2}^T S(v_{r,2})v_{r,1}, & t_{f,1} \leq t < t_c, \\ -k_{c,3}\Phi_3\bar{v}_{r,d,3}^T S(v_{r,2})v_{r,1}, & t \geq t_c. \end{cases} \tag{39b}$$

In (39a)-(39b), $k_{c,1} > 0$, $k_{c,2} > 0$, $k_{c,3} > 0$, $\Phi_1 \triangleq \Phi(\frac{\varphi_1}{\rho_1})$, $\Phi_2 \triangleq \Phi(\frac{\varphi_2}{\rho_2})$, $\Phi_3 \triangleq \Phi(\frac{\varphi_3}{\rho_3})$, $G^\dagger$ is the pseudo inverse of the matrix G, and η is defined in (5).

Correspondingly, the sliding variable is denoted by

$$w_r \triangleq w_{er} - w_c. \tag{40}$$

When $t \geq t_{f,1}$, it is obtained from (38), (40), $w_{er} = w - \bar{w}_d$ and $v_{r,1} = Qv_{b,1}$ that

$$\begin{aligned} S(v_{r,1})Qw &= S(v_{r,1})Q(w_r + \bar{w}_d + w_{c,1} + \lambda_c v_{b,1}) \\ &= S(v_{r,1})Q(w_r + \bar{w}_d + w_{c,1}). \end{aligned} \tag{41}$$

Then, for the error function φ_1, the associated Lyapunov function candidate is constructed as $V_{k,1} \triangleq W_e(\frac{\varphi_1}{\rho_1})$, where the function $W_e(\cdot)$ is defined in (9). According to (10)-(11), (19)-(20), (22), (27a), (38)-(39a), (40)-(41), Lemma 5 and the Young's inequality, if the constraint (28) is satisfied, the derivative of $V_{k,1}$ is scaled as

$$\begin{aligned} \dot{V}_{k,1} =& -\frac{k_{c,1}\Phi_1^2}{\eta^4\rho_1}\|x_{er}\|^2 - \frac{\Phi_1}{\eta^2\rho_1}x_{er}^T G w_r - \frac{\Phi_1}{\rho_1}x_{er}^T\dot{x}_d \\ &- \frac{\dot{\rho}_1\Phi_1}{2\rho_1^2}\|x_{er}\|^2 - \frac{\Phi_1}{\eta^2\rho_1}x_{er}^T G Q_{er}^T w_d \\ \leq& -\frac{5k_{c,1}\Phi_1^2}{8\eta^4\rho_1}\|x_{er}\|^2 + \frac{4\lambda_{G,max}}{k_{c,1}\rho_1}\|w_r\|^2 \\ &+ \frac{4\lambda_{G,max}}{k_{c,1}\rho_1}\|w_d\|^2 + \frac{2\eta^4}{k_{c,1}\rho_1}\|\dot{x}_d\|^2 + \frac{\dot{\rho}_1^2\eta^4}{2k_{c,1}\rho_1^3}\|x_{er}\|^2. \end{aligned} \tag{42}$$

Besides, when $\varphi_3(t_{f,1}) > 2-\epsilon_1$, the Lyapunov function candidate on φ_2 is set in $[t_{f,1}, t_{f,1}+t_{f,2})$ as $V_{k,2} \triangleq W_e(\frac{\varphi_2}{\rho_2})$. Based on (10)-(11), (15a), (25a), (26a), (27b), (38), (39a)-(39b), (40)-(41) and $v_{r,1} = Qv_{b,1}$, if the constraints (28) and (30) hold in $[t_{f,1}, t_{f,1}+t_{f,2})$, the derivative of $V_{k,2}$ is

$$\begin{aligned} \dot{V}_{k,2} =& \frac{\Phi_2}{\rho_2}\bar{v}_{r,d,2}^T S(v_{r,2})Q(w_r + \bar{w}_d) \\ &- \frac{k_{c,2}\Phi_2^2}{\rho_2}(1-(\bar{v}_{r,d,2}^T v_{r,2})^2) - \Phi_2\frac{\dot{\rho}_2}{\rho_2^2}(1-\bar{v}_{r,d,2}^T v_{r,2}) \\ &+ \frac{k_{c,1}\Phi_2}{\rho_2\eta^2}\bar{v}_{r,d,2}^T S(v_{r,2})QG^\dagger\Phi_1 x_{er} \\ &+ \frac{\Phi_2}{\rho_2\|\tilde{v}_{r,d,2}\|}v_{r,2}^T\Psi_2 S(v_{r,1})S(v_{r,d,2})Q_d w_d \\ &- \frac{\Phi_2}{\rho_2\|\tilde{v}_{r,d,2}\|}v_{r,2}^T\Psi_2 S(v_{r,d,2})S(v_{r,1})Q(w_r + \bar{w}_d) \\ &- \frac{k_{c,1}\Phi_1\Phi_2}{\rho_2\eta^2\|\tilde{v}_{r,d,2}\|}v_{r,2}^T\Psi_2 S(v_{r,d,2})S(v_{r,1})QG^\dagger x_{er}. \end{aligned} \tag{43}$$

Based on the Young's inequality, (36) and Lemma 5, the derivative of $V_{k,2}$ (43) is scaled as

$$\begin{aligned}\dot{V}_{k,2} \leq & -\frac{k_{c,2}\Phi_2^2}{4\rho_2}(1-(\bar{v}_{r,d,2}^T v_{r,2})^2)+\frac{c_1}{\rho_2}\|w_r\|^2 \\ & +\frac{c_2\Phi_1^2}{\rho_2\eta^4}\|x_{er}\|^2+\frac{c_3}{\rho_2}\|w_d\|^2 \\ & +\frac{2\dot{\rho}_2^2(1-\bar{v}_{r,d,2}^T v_{r,2})}{k_{c,2}\rho_2^3(1+\bar{v}_{r,d,2}^T v_{r,2})},\end{aligned} \tag{44}$$

if the constraints (28) and (30) hold, where $c_1 \triangleq \frac{4}{k_{c,2}}(\frac{1}{(1-\rho_{\infty,1})^2}+1)$, $c_2 \triangleq \frac{2k_{c,1}^2}{k_{c,2}\lambda_{G,min}}(1+\frac{1}{(1-\rho_{\infty,1})^2})$ and $c_3 \triangleq \frac{2}{k_{c,2}}(2+\frac{3}{(1-\rho_{\infty,1})^2})$.

Additionally, in the time interval $[t_c,+\infty)$, the Lypuanov function candidate on φ_3 is constructed as $V_{k,3} \triangleq W_e(\frac{\varphi_3}{\rho_3})$. According to (10)-(11), (15a), (25b), (26b), (27c), (38), (39a)-(39b), (40), (41) and $v_{r,1}=Qv_{b,1}$, if the constraints (28) and (31) hold in $[t_c,+\infty)$, the derivative of $V_{k,3}$ is

$$\begin{aligned}\dot{V}_{k,3} = & \frac{\Phi_3}{\rho_3}\bar{v}_{r,d,3}^T S(v_{r,2})Q(w_r+\bar{w}_d)-\Phi_3\frac{\dot{\rho}_3}{\rho_3^2}(1-\bar{v}_{r,d,3}^T v_{r,2}) \\ & -\frac{k_{c,3}\Phi_3^2}{\rho_3}(1-(\bar{v}_{r,d,3}^T v_{r,2})^2) \\ & +\frac{k_{c,1}\Phi_1\Phi_3}{\rho_3\eta^2}\bar{v}_{r,d,3}^T S(v_{r,2})QG^\dagger x_{er} \\ & -\frac{\Phi_3}{\rho_3\|\tilde{v}_{r,d,3}\|}v_{r,2}^T\Psi_3\Psi_4 Q(w_r+\bar{w}_d) \\ & -\frac{k_{c,1}\Phi_1\Phi_3}{\rho_3\|\tilde{v}_{r,d,3}\|\eta^2}v_{r,2}^T\Psi_3\Psi_4 QG^\dagger x_{er} \\ & +\frac{\Phi_3}{\rho_3\|\tilde{v}_{r,d,3}\|}v_{r,2}^T\Psi_3(E_3-v_{r,1}v_{r,1}^T)S(v_{r,d,2})Q_d w_d.\end{aligned} \tag{45}$$

Notice that

$$\Psi_4^T\Psi_4 \leq 4(v_{r,1}^T v_{r,d,3})^2 E_3 \leq 4E_3. \tag{46}$$

Based on the Young's inequality, (36), (46) and Lemma 5, the derivative of $V_{k,3}$ (45) is scaled as

$$\begin{aligned}\dot{V}_{k,3} \leq & -\frac{k_{c,3}\Phi_3^2}{4\rho_3}(1-(v_{r,2}^T\bar{v}_{r,d,3})^2)+\frac{c_4}{\rho_3}\|w_r\|^2 \\ & +\frac{c_5\Phi_1^2}{\rho_3\eta^4}\|x_{er}\|^2+\frac{c_6}{\rho_3}\|w_d\|^2 \\ & +\frac{2\dot{\rho}_3^2(1-\bar{v}_{r,d,3}^T v_{r,2})}{k_{c,3}\rho_3^3(1+\bar{v}_{r,d,3}^T v_{r,2})},\end{aligned} \tag{47}$$

if the constraints (28) and (31) hold, where $c_4 \triangleq \frac{4}{k_{c,3}}(1+\frac{4}{(1-\rho_{\infty,1})^2})$, $c_5 \triangleq \frac{2k_{c,1}^2}{k_{c,3}\lambda_{G,min}}(1+\frac{4}{(1-\rho_{\infty,1})^2})$, $c_6 \triangleq \frac{2}{k_{c,3}}(2+\frac{9}{(1-\rho_{\infty,1})^2})$.

Moreover denote

$$V_k \triangleq \begin{cases} V_{k,1}, & 0 \leq t < t_{f,1}; \\ V_{k,1}+c_7V_{k,2}, & t_{f,1} \leq t < t_c; \\ V_{k,1}+c_8V_{k,3}, & t \geq t_c, \end{cases} \tag{48}$$

where $c_7 \triangleq \frac{k_{c,1}\rho_{\infty,2}}{8c_2\rho_{0,1}}$ and $c_8 \triangleq \frac{k_{c,1}\rho_{\infty,3}}{8c_5\rho_{0,1}}$. On one hand, when $t_{f,1} \leq t < t_c$, it is obtained from (8) that $\dot{\rho}_1(t)=0$ and, together with (42) and (44), that the derivative of $V_k = V_{k,1}+c_7V_{k,2}$ is scaled as

$$\begin{aligned}\dot{V}_k \leq & -\frac{k_{c,1}\Phi_1^2}{2\eta^4\rho_1}\|x_{er}\|^2-\frac{k_{c,2}c_7\Phi_2^2}{4\rho_2}(1-(v_{r,2}^T\bar{v}_{r,d,2})^2) \\ & +(\frac{4\lambda_{G,max}}{k_{c,1}\rho_1}+\frac{c_1c_7}{\rho_2})\|w_r\|^2+\frac{2\eta^4}{k_{c,1}\rho_1}\|\dot{x}_d\|^2 \\ & +(\frac{c_3c_7}{\rho_2}+\frac{4\lambda_{G,max}}{k_{c,1}\rho_1})\|w_d\|^2+\frac{2c_7\dot{\rho}_2^2(1-v_{r,2}^T\bar{v}_{r,d,2})}{k_{c,2}\rho_2^3(1+v_{r,2}^T\bar{v}_{r,d,2})},\end{aligned} \tag{49}$$

if the constraints (28) and (30) hold. On the other hand, if $t \geq t_c$, it can be also obtained from (8) that $\dot{\rho}_1(t)=0$. Hence, based upon (42) and (47), if the constraints (28) and (31) hold, the derivative of $V_k = V_{k,1}+c_8V_{k,3}$ is bounded as

$$\begin{aligned}\dot{V}_k \leq & -\frac{k_{c,1}\Phi_1^2}{2\eta^4\rho_1}\|x_{er}\|^2-\frac{k_{c,3}c_8\Phi_3^2}{4\rho_3}(1-(v_{r,2}^T\bar{v}_{r,d,3})^2) \\ & +(\frac{4\lambda_{G,max}}{k_{c,1}\rho_1}+\frac{c_4c_8}{\rho_3})\|w_r\|^2+\frac{2\eta^4}{k_{c,1}\rho_1}\|\dot{x}_d\|^2 \\ & +(\frac{c_6c_8}{\rho_3}+\frac{4\lambda_{G,max}}{k_{c,1}\rho_1})\|w_d\|^2+\frac{2c_8\dot{\rho}_3^2(1-\bar{v}_{r,d,3}^T v_{r,2})}{k_{c,3}\rho_3^3(1+\bar{v}_{r,d,3}^T v_{r,2})}.\end{aligned} \tag{50}$$

D. Control Input Design

Based upon the designed virtual controller (38) and (39a)-(39b), the actual control input will be put forward in this subsection. First, in view of (14b) and (40), it is obtained that

$$J\dot{w}_r = (S(Jw)-S(\bar{w}_d)J-JS(\bar{w}_d))w_r+\tau+\Xi_1, \tag{51}$$

where

$$\begin{aligned}\Xi_1 = & -J\dot{w}_c-S(\bar{w}_d)J\bar{w}_d-JQ_{er}^T a_d+S(Jw)w_c \\ & -(S(\bar{w}_d)J+JS(\bar{w}_d))w_c+d.\end{aligned} \tag{52}$$

The Lyapunov function candidate on w_r is $V_{w,r}=\frac{1}{2}w_r^TJw_r$, and in view of (51), and its derivative is

$$\dot{V}_{w,r} = w_r^T\tau+w_r^T\Xi_1. \tag{53}$$

Notice that $\Xi_1(t)$ is the term on the uncertain inertia parameters and the external disturbances, and in view of Property 1 and the Young's inequality, it follows that

$$\begin{aligned}w_r^T\Xi_1 \leq & \frac{\lambda_{J,max}^2}{2\epsilon_2}\|w_d\|^2\|w_c\|^2\|w_r\|^2+\frac{\lambda_{J,max}^2}{4\epsilon_2}\|\dot{w}_c\|^2\|w_r\|^2 \\ & +\frac{\lambda_{J,max}^2}{4\epsilon_2}\|w\|^2\|w_c\|^2\|w_r\|^2+3\epsilon_2 \\ & -w_r^TS(\bar{w}_d)J\bar{w}_d-w_r^TJQ_{er}^Ta_d+w_r^Td.\end{aligned} \tag{54}$$

Correspondingly, it follows from (53)-(54) that

$$\begin{aligned}\dot{V}_{w,r} \leq & w_r^T(-S(\bar{w}_d)J\bar{w}_d-JQ_{er}^Ta_d+d)+3\epsilon_2 \\ & +\frac{\lambda_{J,max}^2}{2\epsilon_2}\|w_d\|^2\|w_c\|^2\|w_r\|^2+\frac{\lambda_{J,max}^2}{4\epsilon_2}\|\dot{w}_c\|^2\|w_r\|^2 \\ & +\frac{\lambda_{J,max}^2}{4\epsilon_2}\|w\|^2\|w_c\|^2\|w_r\|^2+w_r^T\tau,\end{aligned} \tag{55}$$

where $\epsilon_2 > 0$. Owing to the uniform boundedness of $w_d(t)$ and $a_d(t)$, it follows that there exist two constants $\Delta_1 > 0$ and $\Delta_2 > 0$ such that $\| - S(\bar{w}_d(t))J\bar{w}_d(t) - JQ_{er}^T(t)a_d(t) + d(t)\| \leq \lambda_{J,max}\|w_d(t)\|^2 + \lambda_{J,max}\|a_d(t)\| + \|d(t)\| < \Delta_1$ and $\frac{\lambda_{J,max}^2}{2\epsilon_2}\|w_d(t)\|^2 + \frac{\lambda_{J,max}^2}{4\epsilon_2} < \Delta_2$. Correspondingly, based upon the relation $\|w_r\| \leq w_r^T \tanh(\frac{1}{\epsilon_3}w_r) + 3\epsilon_3\delta_1$ with $\epsilon_3 > 0$ and $\delta_1 = 0.2785$ [62], it is further obtained from (55) that

$$\begin{aligned}\dot{V}_{w,r} \leq & w_r^T \tanh(\frac{1}{\epsilon_3}w_r)\Delta_1 + 3\epsilon_3\delta_1\Delta_1 + w_r^T\tau + 3\epsilon_2 \\ & + \Delta_2(\|\dot{w}_c\|^2 + \|w_c\|^2 + \|w_c\|^2\|w\|^2)\|w_r\|^2.\end{aligned} \tag{56}$$

Then, the control input is designed as

$$\begin{aligned}\tau = & - k_{w,c}w_r - r_{u,1}\tanh(\frac{1}{\epsilon_3}w_r) \\ & - r_{u,2}(\|\dot{w}_c\|^2 + \|w_c\|^2 + \|w_c\|^2\|w\|^2)w_r,\end{aligned} \tag{57}$$

where $k_{w,c} > 0$, $r_{u,1}(t)$ and $r_{u,2}(t)$ are dynamic gaining variables satisfying the following equations

$$\dot{r}_{u,1} = \Gamma_{u,1}w_r^T \tanh(\frac{1}{\epsilon_3}w_r) - k_{u,1}r_{u,1}, \tag{58a}$$

$$\begin{aligned}\dot{r}_{u,2} = & \Gamma_{u,2}(\|\dot{w}_c\|^2 + \|w_c\|^2 + \|w_c\|^2\|w\|^2)\|w_r\|^2 \\ & - k_{u,2}r_{u,2},\end{aligned} \tag{58b}$$

with the parameters $\Gamma_{u,1} > 0$, $\Gamma_{u,2} > 0$, $k_{u,1} > 0$ and $k_{u,2} > 0$ and the function $\tanh(\cdot)$ defined in Notations. Here $r_{u,1}(0) \geq 0$, $r_{u,2}(0) \geq 0$, and according to (58a)-(58b), it is obtained that $r_{u,1}(t) \geq 0$ and $r_{u,2}(t) \geq 0$. Denote $V_{u,1} \triangleq \frac{1}{2\Gamma_{u,1}}(r_{u,1} - \Delta_1)^2$, $V_{u,2} \triangleq \frac{1}{2\Gamma_{u,2}}(r_{u,2} - \Delta_2)^2$ and $V_d \triangleq V_{w,r} + V_{u,1} + V_{u,2}$, and based upon (56), (57), (58a)-(58b), and the Young's inequality, the derivative of V_d is bounded as

$$\dot{V}_d \leq - k_{w,c}\|w_r\|^2 - \frac{3k_{u,1}}{2}V_{u,1} - \frac{3k_{u,2}}{2}V_{u,2} + \acute{\Delta}_c, \tag{59}$$

where $\acute{\Delta}_c \triangleq 3\epsilon_3\delta_1\Delta_1 + 3\epsilon_2 + \frac{k_{u,1}\Delta_1^2}{\Gamma_{u,1}} + \frac{k_{u,2}\Delta_2^2}{\Gamma_{u,2}}$. In addition, denote $V_c \triangleq V_k + c_9V_d$, where $c_9 \triangleq \frac{2}{k_{w,c}}\{\frac{4\lambda_{G,max}}{k_{c,1}\rho_{\infty,1}} + \frac{c_1c_7}{\rho_{\infty,2}} + \frac{c_4c_8}{\rho_{\infty,3}}\}$, and it follows from (12), (42), (49)-(50) and (59) that

$$\dot{V}_c \leq -\Pi_c + \Pi_e + \Delta_c, \tag{60}$$

where

$$\begin{aligned}\Pi_c \triangleq & \Pi_{c,1} + \frac{c_9k_{w,c}}{\lambda_{J,max}}V_{w,r} \\ & + \frac{3c_9k_{u,1}}{2}V_{u,1} + \frac{3c_9k_{u,2}}{2}V_{u,2},\end{aligned} \tag{61a}$$

$$\Pi_{c,1} \triangleq \begin{cases} \frac{k_{c,1}\Phi_1}{16}V_{k,1}, & 0 \leq t < t_{f,1}; \\ \frac{k_{c,1}\Phi_1}{16}V_{k,1} + \frac{k_{c,2}c_7\Phi_2(1+v_{r,2}^T\bar{v}_{r,d,2})}{4}V_{k,2}, & t_{f,1} \leq t < t_c; \\ \frac{k_{c,1}\Phi_1}{16}V_{k,1} + \frac{k_{c,3}c_8\Phi_3(1+v_{r,2}^T\bar{v}_{r,d,3})}{4}V_{k,3}, & t \geq t_c, \end{cases} \tag{61b}$$

$$\Pi_e \triangleq \begin{cases} \frac{8\dot{\rho}_1^2}{k_{c,1}\rho_1^3}\|x_{er}\|^2, & 0 \leq t < t_{f,1}; \\ \frac{2c_7\rho_2^2(1-\bar{v}_{r,d,2}^Tv_{r,2})}{k_{c,2}\rho_2^3(1+\bar{v}_{r,d,2}^Tv_{r,2})}, & t_{f,1} \leq t < t_c; \\ \frac{2c_8\rho_3^2(1-\bar{v}_{r,d,3}^Tv_{r,2})}{k_{c,3}\rho_3^3(1+\bar{v}_{r,d,3}^Tv_{r,2})}, & t \geq t_c, \end{cases} \tag{61c}$$

and $\Delta_c(t) \triangleq c_9\acute{\Delta}_c + \frac{32\|\dot{x}_d\|^2}{k_{c,1}\rho_{\infty,1}} + (\frac{4\lambda_{G,max}}{k_{c,1}\rho_{\infty,1}} + \frac{c_3c_7}{\rho_{\infty,2}} + \frac{c_6c_8}{\rho_{\infty,3}})\|w_d\|^2$. Notice that $\Pi_{c,1}(t) \geq 0$, $\Pi_c(t) \geq 0$, $\Pi_e(t) \geq 0$, and $\Delta_c(t)$ is uniformly bounded at all the time.

Then the following theorem is obtained.

Theorem 1: For the control scheme (38), (39a)-(39b), (40), (57), and (58a)-(58b), if the initial spacecraft attitude meets the constraints (4) and (28), $r_{u,1}(0) \geq 0$ and $r_{u,2}(0) \geq 0$, then the variables $Q_{er}(t)$, $w(t)$, $r_{u,1}(t)$ and $r_{u,2}(t)$ are all uniformly bounded with $r_{u,1}(t) \geq 0$ and $r_{u,2}(t) \geq 0$. Besides, the constraint (4) is satisfied at all the time, and $Q_{er}(t)$ can fall into the set Θ_R (32) with the setting time $\bar{t}_f$ s. ■

Proof: The proof of this theorem includes four steps.

a). The uniform boundedness of $V_c(t)$ in $[0, t_{f,1})$.

First, it will be proved by contradiction that the function $V_{k,1}(t)$ is uniformly bounded in $[0, t_{f,1})$. Suppose that the above claim is invalid. Hence there is a time instant $t_{h,1} \in (0, t_{f,1})$ so that $\lim_{t\to t_{h,1}^-} V_{k,1}(t) = +\infty$ and $V_{k,1}(t)$ is finite for any $t \in [0, t_{h,1})$. It follows from (9) that the constraint (28) is satisfied in $[0, t_{h,1})$, and $x_{er}(t)$ is uniformly bounded in $[0, t_{h,1})$. Then according to (59), it is obtained that $w_r(t)$, $r_{u,1}(t)$, $r_{u,2}(t)$ and $V_d(t)$ are all uniformly bounded in $[0, t_{h,1})$. Based on the uniform boundedness of $x_{er}(t)$, $w_r(t)$, $\dot{x}_d(t)$ and $w_d(t)$ in $[0, t_{h,1})$, it follows from (42) that $V_{k,1}(t)$ is uniformly bounded in $[0, t_{h,1})$, which contradicts with the above assumption. Hence, the above assumption is invalid, meaning that in the time interval $[0, t_{f,1})$, $V_{k,1}(t)$ is uniformly bounded, the constraints (4) and (28) hold, and $x_{er}(t)$, $\Phi_1(t)$, $G^\dagger(t)$ and $w_c(t) = w_{c,1}(t)$ (39a) are all uniformly bounded.

Then, it will be verified that $V_c(t)$ is uniformly bounded in $[0, t_{f,1})$. First, since the constraint (28) holds in $[0, t_{f,1})$, Eq. (60) holds in $[0, t_{f,1})$. From (7)-(8), it follows that $\rho_1(t) \geq \rho_{\infty,1}$, $\dot{\rho}_1(t)$ is uniformly bounded and, together with the uniform boundedness of $x_{er}(t)$ in $[0, t_{f,1})$, that $\Pi_e(t)$ is uniformly bounded in $[0, t_{f,1})$. Since $\Delta_c(t)$ is uniformly bounded, it follows from (60) that $V_c(t)$ is also uniformly bounded in $[0, t_{f,1})$, meaning that $Q_{er}(t)$, $w_r(t)$, $r_{u,1}(t)$ and $r_{u,2}(t)$ are all uniformly bounded in $[0, t_{f,1})$. Besides, due to the uniform boundedness of $w_r(t)$, $w_c(t)$ and $\bar{w}_d(t)$ in $[0, t_{f,1})$, it follows that $w(t)$ is also uniformly bounded in $[0, t_{f,1})$.

b). The uniform boundedness of $V_c(t)$ in $[t_{f,1}, t_c)$ when $\varphi_3(t_{f,1}) > 2 - \epsilon_1$.

First, if $\varphi_3(t_{f,1}) = 1 - \bar{v}_{r,d,3}^T(t_{f,1})v_{r,2}(t_{f,1}) > 2 - \epsilon_1$, it is obtained from (29a)-(29b) and Remark 5 that $t_c = t_{f,1} + t_{f,2}$, $\bar{t}_f = t_{f,1} + t_{f,2} + t_{f,3}$, and the constraint (30) holds when $t = t_{f,1}$. Accordingly, it is obtained that $V_{k,2}(t_{f,1}) < +\infty$.

Besides, similar to the proof procedure of part a), it follows that in the time interval $[t_{f,1}, t_{f,1} + t_{f,2})$, $V_{k,1}(t)$ is uniformly bounded, the constraints (4) and (28) always hold, and $x_{er}(t)$, $\Phi_1(t)$, $G^\dagger(t)$ and $w_{c,1}(t)$ are also uniformly bounded.

Then it will be proved by contradiction that $V_{k,2}(t)$ is uniformly bounded in $[t_{f,1}, t_{f,1} + t_{f,2})$. Suppose the above claim is invalid. Notice that $V_{k,2}(t_{f,1}) < +\infty$, and hence there exists a time instant $t_{h,2} \in (t_{f,1}, t_{f,1} + t_{f,2})$ so that $\lim_{t\to t_{h,2}^-} V_{k,2}(t) = +\infty$ and $V_{k,2}(t) < +\infty$ when $t \in [t_{f,1}, t_{h,2})$. From (59), it is obtained that $w_r(t)$, $r_{u,1}(t)$ and $r_{u,2}(t)$ are all uniformly bounded in $[t_{f,1}, t_{h,2})$, and it is also obtained from the uniform boundedness of $V_{k,1}(t)$ in

$[t_{f,1}, t_{f,1}+t_{f,2})$ that the term $\frac{c_2\Phi_1^2(t)}{\rho_2(t)\eta^4(t)}\|x_{er}(t)\|^2$ in (44) is also uniformly bounded in $[t_{f,1}, t_{f,1}+t_{f,2})$. Moreover, since $V_{k,2}(t) < +\infty$ in $[t_{f,1}, t_{h,2})$, it is obtained that the constraint (30) holds in $[t_{f,1}, t_{h,2})$, $1+v_{r,2}^T(t)\bar{v}_{r,d,2}(t) > 2-\rho_{0,2} > 0$ in $[t_{f,1}, t_{h,2})$, and

$$\frac{k_{c,2}\Phi_2^2}{4\rho_2}(1-(\bar{v}_{r,d,2}^T v_{r,2})^2) \geq \frac{k_{c,2}(2-\rho_{0,2})}{4}V_{k,2}, \tag{62a}$$

$$\frac{2\dot{\rho}_2^2(1-\bar{v}_{r,d,2}^T v_{r,2})}{k_{c,2}\rho_2^3(1+\bar{v}_{r,d,2}^T v_{r,2})} \leq \frac{4\dot{\rho}_2^2}{k_{c,2}\rho_2^3(2-\rho_{0,2})}. \tag{62b}$$

Based upon the uniformly boundedness of $\frac{c_2\Phi_1^2(t)}{\rho_2(t)\eta^4(t)}\|x_{er}(t)\|^2$, $w_r(t)$, $w_d(t)$, and Eqs. (44) and (62a)-(62b), it is obtained that $V_{k,2}(t)$ is uniformly bounded in $[t_{f,1}, t_{h,2})$, which contradicts with the above assumption. Hence, the above assumption is invalid, and $V_{k,2}(t)$ is uniformly bounded in $[t_{f,1}, t_{f,1}+t_{f,2})$. This means that in the time interval $[t_{f,1}, t_{f,1}+t_{f,2})$, $\varphi_2(t)$ meets the constraint (30) and is uniformly bounded with $\varphi_2(t_{f,1}+t_{f,2}) < \rho_{\infty,2}$, and both $\Phi_2(t)$ and $\lambda_c(t)$ (39b) are also uniformly bounded. Due to the unform boundedness of $w_{c,1}(t)$ and $\lambda_c(t)$ in $[t_{f,1}, t_{f,1}+t_{f,2}]$, it follows that $w_c(t)$ (38) is also uniformly bounded in $[t_{f,1}, t_{f,1}+t_{f,2}]$.

Additionally, similar to the proof procedure of part a), it is obtained that in $V_c(t)$ is uniformly bounded in $[t_{f,1}, t_{f,1}+t_{f,2})$. Correspondingly, $Q_{er}(t)$, $w_r(t)$, $r_{u,1}(t)$, $r_{u,2}(t)$, $w_c(t)$ and $w(t)$ are all uniformly bounded in $[t_{f,1}, t_{f,1}+t_{f,2})$.

c). The uniform boundedness of $V_c(t)$ in $[t_c, +\infty)$.

First, it will be proved that $V_{k,3}(t_c) < +\infty$. On one hand, if $\varphi_3(t_{f,1}) \leq 2-\epsilon_1$, it is obtained from (29a)-(29b) and Remark 5 that $t_c = t_{f,1}$, $\bar{t}_f = t_{f,1}+t_{f,3}$ and $\varphi_3(t_c)$ meets the constraint (31), meaning that $V_{k,3}(t_c) < +\infty$. On the other hand, if $\varphi_3(t_{f,1}) > 2-\epsilon_1$, it can be also obtained from (29a)-(29b) and the proof procedure of part b) that $t_c = t_{f,1}+t_{f,2}$, $\bar{t}_f = t_{f,1}+t_{f,2}+t_{f,3}$, and $\varphi_2(t_{f,1}+t_{f,2}) < \rho_{\infty,2}$. Accordingly, it follows from Remark 5 that $\varphi_3(t_c)$ also meets the constraint (31) and $V_{k,3}(t_c) < +\infty$. In all, it is obtained that $V_{k,3}(t_c) < +\infty$.

Besides, based upon the similar proof procedure of part a), it is obtained that $V_{k,1}(t)$ is uniformly bounded in $[t_c, +\infty)$. This means that in the time interval $[t_c, +\infty)$, $\varphi_1(t) < \rho_{\infty,1}$, $x_{er}(t)$ and $\Phi_1(t)$ are both uniformly bounded, the attitude constraint (4) always holds, $G^\dagger(t)$ is uniformly bounded, and $w_{c,1}(t)$ (39a) is also uniformly bounded.

Then it will be verified by contradiction that the function $V_{k,3}(t)$ is uniformly bounded in $[t_c, +\infty)$. Suppose that this claim is invalid, which implies that there exists a time instant $t_{h,3}$ with $t_c < t_{h,3} \leq +\infty$, such that $\lim_{t\to t_{h,3}^-} V_{k,3}(t) = +\infty$ and $V_{k,3}(t) < +\infty$ when $t \in [t_c, t_{h,3})$. Similar to the proof procedure of part a), it is obtained that $w_r(t)$, $r_{u,1}(t)$ and $r_{u,2}(t)$ are all uniformly bounded in $[t_c, t_{h,3})$. Besides, since in the time interval $[t_c, +\infty)$, $x_{er}(t)$ and $\Phi_1(t)$ are both uniformly bounded, $\rho_3(t) \geq \rho_{\infty,3}$, and the attitude constraint (4) always holds, it is obtained that the term $\frac{c_5\Phi_1^2(t)}{\rho_3(t)\eta^4(t)}\|x_{er}(t)\|^2$ in (47) is uniformly bounded in $[t_c, +\infty)$. Moreover, since $V_{k,3}(t) < +\infty$ in $[t_c, t_{h,3})$, it is obtained that in $[t_c, t_{h,3})$, the constraint (31) is satisfied and $1+v_{r,2}^T(t)\bar{v}_{r,d,3}(t) > 2-\rho_{0,3} > 0$. Correspondingly, in view of (12), it follows that

$$\frac{k_{c,3}}{4\rho_3}\Phi_3^2(1-(v_{r,2}^T\bar{v}_{r,d,3})^2) \geq \frac{k_{c,3}(2-\rho_{0,3})}{4}V_{k,3}, \tag{63a}$$

$$\frac{2\dot{\rho}_3^2(1-\bar{v}_{r,d,3}^T v_{r,2})}{k_{c,3}\rho_3^3(1+\bar{v}_{r,d,3}^T v_{r,2})} \leq \frac{4\dot{\rho}_3^2}{k_{c,3}\rho_3^3(2-\rho_{0,3})}. \tag{63b}$$

Based on the uniform boundedness of $w_r(t)$, $w_d(t)$ and $\frac{c_5}{\rho_3(t)\eta^4(t)}\Phi_1^2(t)\|x_{er}(t)\|^2$, and Eqs. (47) and (63a)-(63b), it follows that $V_{k,3}(t)$ is uniformly bounded in $[t_c, t_{h,3})$, which contradicts with the previous assumption. Hence, the previous assumption is invalid, and $V_{k,3}(t)$ is uniformly bounded in $[t_c, +\infty)$, which means that in the time interval $[t_c, +\infty)$, the constraint (31) holds, $\varphi_3(t)$ and $\Phi_3(t)$ are both uniformly bounded, and $\lambda_c(t)$ (39b) is also uniformly bounded. Due to the uniform boundedness of $w_{c,1}(t)$ and $\lambda_c(t)$ in $[t_c, +\infty)$, it follows that $w_c(t)$ (38) is also uniformly bounded in $[t_c, +\infty)$.

In addition, it will be verified that $V_c(t)$ is uniformly bounded in $[t_c, +\infty)$. First, since $V_{k,1}(t)$ and $V_{k,3}(t)$ are both uniformly bounded in $[t_c, +\infty)$, it follows that Eq. (60) holds in $[t_c, +\infty)$. It can be seen in (61c) and (63b) that $\Pi_e(t)$ is uniformly bounded in $[t_c, +\infty)$. Besides, it follows from $\Phi_1(t) \geq 1$, (61a)-(61b) and (63a) that in $[t_c, +\infty)$,

$$\Pi_c \geq \bar{c}_1 V_c, \tag{64}$$

where $\bar{c}_1 \triangleq \max(\frac{k_{c,1}}{16}, \frac{k_{c,3}(2-\rho_{0,3})}{4}, \frac{k_{w,c}}{\lambda_{J,max}}, k_{u,1}, k_{u,2}) > 0$. Hence, based on (60), (64), and the uniform boundedness of $\Pi_e(t)$ and $\Delta_c(t)$ in $[t_c, +\infty)$, it follows that $V_c(t)$ is uniformly bounded in $[t_c, +\infty)$. This means that in $[t_c, +\infty)$, $Q_{er}(t)$, $w_r(t)$, $r_{u,1}(t)$, $r_{u,2}(t)$ and $w(t)$ are all uniformly bounded.

d). The prescribed performance of the tracking error $Q_{er}(t)$.

First, based upon the above proof procedure, it is obtained that $V_{k,1}(t)$, $V_c(t)$, $Q_{er}(t)$, $w(t)$, $r_{u,1}(t)$ and $r_{u,2}(t)$ are all uniformly bounded, and the constraints (4) and (28) hold at all the time, which means that $\varphi_1(t) < \rho_{\infty,1}$ when $t \geq t_{f,1}$. Since $V_{k,3}(t)$ is also uniformly bounded in $[t_c, +\infty)$ and the constraint (31) always holds in the time interval $[t_c, +\infty)$, it follows that $\varphi_3(t) < \rho_{\infty,3}$ when $t \geq \bar{t}_f$. Hence, according to Lemma 6, it follows that $Q_{er}(t)$ will always be within the set Θ_R (32) when $t \geq \bar{t}_f$. Moreover, in view of (58a)-(58b), it follows that $r_{u,1}(t) \geq 0$ and $r_{u,2}(t) \geq 0$ at all the time. The proof of Theorem 1 is complete. ■

Remark 7: The distinctions between the proposed control scheme and those in [40]-[44] and [59]-[60] are discussed as follows. First, in this paper, a novel projection function $\Pr(\cdot)$ (17) is designed to map the boresight vector $v_{r,1}(t)$ to a reduced dimensional vector $x(t)$. On one hand, notice that the reduced dimensional vectors $x(t)$, and the according auxiliary vectors $\bar{v}_{r,d,2}(t)$ and $\bar{v}_{r,d,3}(t)$ are located in either $\mathbb{R}^2$ or $\mathbb{R}^3$, and therefore the attitude control scheme constructed based upon the above vectors can circumvent the topological obstruction of the nonlinear manifold $SO(3)$. On the other hand, by means of the designed vectors, the requirement of the satisfaction of the attitude constraint (4) is transformed as the requirement of the uniform boundedness of the reduced dimensional vector $x(t)$, which is shown in Lemma 3. The appointed-time performance requirement of the attitude tracking is transformed as the appointed-time tracking performance

TABLE I: The values of system parameters of the spacecraft

Parameter	Value
J (kg $\cdot$ m^2)	diag(973.4, 424.85, 771.06)
v_f	col(0, 0, 1)
$v_{b,1}$	col(1, 0, 0)
θ_f (rad)	$\frac{\pi}{6}$

TABLE II: The values of the control parameters of the proposed control scheme

Parameter	$\rho_{0,1}$	$\rho_{\infty,1}$	$t_{f,1}$	ϵ_1	$\rho_{0,2}$	$\rho_{\infty,2}$	$t_{f,2}$
Value	30	0.3	25	0.4	1.8	0.2	10
Parameter	$\rho_{0,3}$	$\rho_{\infty,3}$	$t_{f,3}$	ϵ_3	$k_{c,1}$	$k_{c,2}$	$k_{c,3}$
Value	1.8	0.2	15	0.2	0.14	0.14	0.14
Parameter	$\Gamma_{u,1}$	$k_{u,1}$	$\Gamma_{u,2}$	$k_{u,2}$	$k_{w,c}$		
Value	0.01	0.06	0.01	0.06	11		

requirement of the according vectors (that is, the vectors $x(t)$ and $v_{r,2}(t)$ should track the vectors $x_d(t)$ and $\bar{v}_{r,d,3}(t)$ respectively, with the appointed-time control performance), which is shown in Lemma 6.

Besides, based upon the above properties, the according vector-based error functions (27a)-(27c), the appointed-time performance constraints (28) and (30)-(31), and the vector-based switching virtual controller (38)-(39b) are carefully constructed. By means of the above design, it is ensured that the vector $x(t)$ is uniformly bounded, the constraint (28) always holds at all the time, and the vector $v_{r,2}(t)$ can always satisfy the constraint (31) when $t \geq t_c$. This means that the attitude constraint (4) is satisfied at all the time, and the attitude tracking error $Q_{er}(t)$ can always remain in the residual set Θ_R (32) when $t \geq \bar{t}_f$.

In all, based on the designed projection function (17), the appointed-time performance constraints (28) and (30)-(31), and the vector-based switching virtual controller (38)-(39b), the proposed attitude control scheme on $SO(3)$ can meet the attitude constraint and the appointed-time control performance simultaneously, and hence differs from those in [40]-[44] and [59]-[60]. On one hand, the artificial-potential-function-based constrained attitude stabilization schemes in [40]-[44] can ensure the satisfaction of the attitude constraint. However, compared with the proposed control scheme, the control schemes in [40]-[44] cannot achieve appointed-time attitude tracking of the spacecraft. On the other hand, by virtue of the designed $SO(3)$-based prescribed performance constraints, the control schemes in [59]-[60] can ensure the appointed transient and steady control performance. However, compared with the proposed control scheme, the control schemes in [59]-[60] cannot satisfy the attitude constraint (4). ■

Remark 8: In this paper, two dynamic gaining factors $r_{u,1}(t)$ and $r_{u,2}(t)$ are employed into the control input (57). Note that in the dynamic equation (51), there is a term $\Xi_1(t)$ (52) which is related to the uncertain parameters and the external disturbances and will affect the closed-loop stability of the spacecraft attitude. Therefore, in order to deal with the term $\Xi_1(t)$, two dynamic gaining variables $r_{u,1}(t)$ (58a) and $r_{u,2}(t)$ (58b) are constructed to adjust the gaining parameters of the control input. It can be seen in (59)-(60) and Theorem 1 that by means of the designed variables $r_{u,1}(t)$ and $r_{u,2}(t)$, the closed-loop stability of the spacecraft attitude can be guaranteed, and the influence of the parameter uncertainties and the external disturbances (that is, the term $\Xi_1(t)$) is attenuated. This means that, compared with [44] and [59], the spacecraft attitude can possess the appointed-time control performance and meet the attitude constraint, even in the presence of the parameter uncertainties and the external disturbances, without the need to estimate the uncertain parameters. It should be noted that due to the presence of the external disturbances, it is only guaranteed that the attitude tracking error of the spacecraft converges into the according residual set Θ_R (32) with the setting time $\bar{t}_f$ s. ■

Remark 9: Notice that the selection of the vectors $v_{b,2}$ and $v_{b,3}$ can change the values of the error functions $\varphi_2(t)$ and $\varphi_3(t)$, and can also change the value of the control input $u(t)$. However, it is worth mentioning that by means of the designed switching laws (29a)-(29b) and the switching virtual controller (38)-(39b), the design of the functions $\varphi_2(t)$, $\varphi_3(t)$, $\rho_2(t)$ and $\rho_3(t)$ is unaffected by these vectors, and the obtained control scheme can still achieve the appointed-time control performance of the spacecraft and satisfy the attitude constraint, as long as the unit vectors $v_{b,2}$ and $v_{b,3}$ satisfy $v_{b,1}^T v_{b,2} = 0$ and $v_{b,3} = S(v_{b,1})v_{b,2}$. Besides, since the value of the control input $u(t)$ is influenced by the vectors $v_{b,2}$ and $v_{b,3}$, it deserves further investigation on the optimal selection of the vectors $v_{b,2}$ and $v_{b,3}$ in the future. ■

IV. Simulation Results

In the section, the simulation results will be provided to show the effectiveness of the proposed scheme. First, the values of the system parameters refer to [15] and can be seen in Table I. Besides, in this paper, the external disturbances of the spacecraft $d(t)$ include the gravity-gradient torque $d_g(t)$, the aerodynamic torque $d_a(t)$ and the Earth magnetic torque $d_e(t)$. According to [15] and [63]-[65], the form of the above disturbance torques are $d_g = \frac{3\mu}{\|\beta_g\|^5} S(\beta_g) J \beta_g$, $d_a = -\frac{1}{2} c_D s_D \varrho_a S(L_p) \|V_a\| V_a$, and $d_e = S(M_e) B_e$, where $\mu = 3.9787 * 10^{14}$ m^{3}s^{-2} is the Earth's gravitational constant, $\beta_g \in \mathbb{R}^3$ is the relative position from the center of the Earth to the spacecraft centroid in $\mathcal{F}_b$, ϱ_a is the atmospheric density, s_D is the area of the spacecraft cross-section, c_D is the drag coefficient, $L_p \in \mathbb{R}^3$ is the relative position from the spacecraft centroid to the center of the pressure in $\mathcal{F}_b$, $V_a \in \mathbb{R}^3$ is the spacecraft velocity in $\mathcal{F}_b$, $B_e \in \mathbb{R}^3$ is geocentric magnetic flux density in $\mathcal{F}_b$, and $M_e \in \mathbb{R}^3$ is the sum of the magnetic moments due to permanent, spacecraft-generated current loops and induced magnetism in $\mathcal{F}_b$. The values of the above parameters and vectors can be seen in [15].

In addition, here the spacecraft is subject to the measurement noises. Correspondingly, denote $Q_m(t) \triangleq Q(t)Q_{dis}(t) \in SO(3)$ and $w_m(t) = w(t) + w_{dis}(t) \in \mathbb{R}^3$ as the measured attitude and the measured angular velocity of the spacecraft, respectively, where $Q_{dis}(t) = E_3 + \frac{\sin(\|\phi_R(t)\|)}{\|\phi_R(t)\|} S(\phi_R(t)) + \frac{1-\cos(\|\phi_R(t)\|)}{\|\phi_R(t)\|^2} S^2(\phi_R(t)) \in SO(3)$ and $w_{dis}(t) = 0.002 * \mathrm{rand}(t) 1_3 \in \mathbb{R}^3$ are the measurement noises of the spacecraft attitude and the spacecraft angular velocity respectively, with $\phi_R(t) = 0.005 * \mathrm{rand}(t) 1_3 \in \mathbb{R}^3$. Notice that the spacecraft

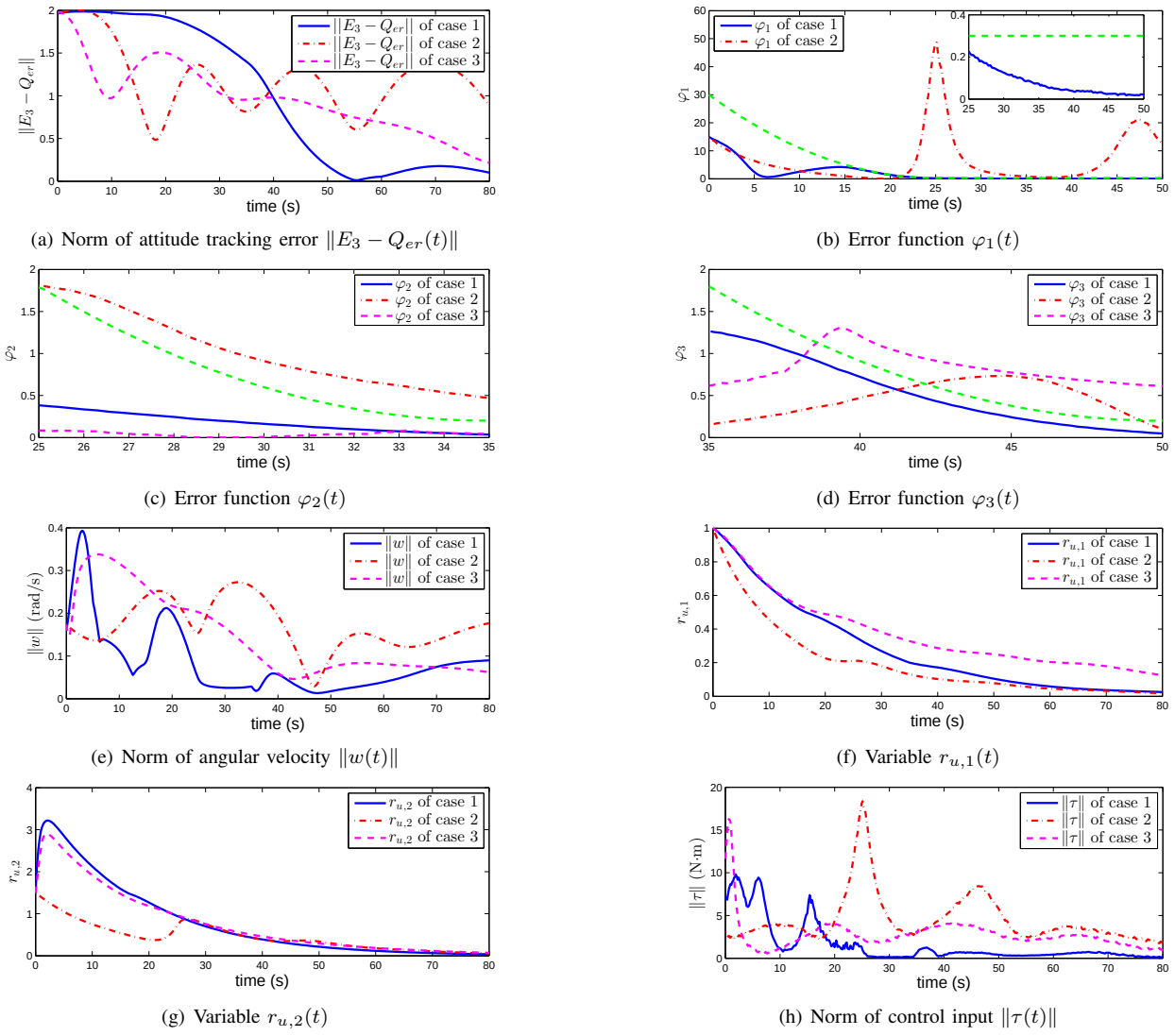

(a) Norm of attitude tracking error $\|E_3 - Q_{er}(t)\|$

(b) Error function $\varphi_1(t)$

(c) Error function $\varphi_2(t)$

(d) Error function $\varphi_3(t)$

(e) Norm of angular velocity $\|w(t)\|$

(f) Variable $r_{u,1}(t)$

(g) Variable $r_{u,2}(t)$

(h) Norm of control input $\|\tau(t)\|$

Fig. 1: Simulation results of three control schemes. Case 1: The proposed scheme. Case 2: The first compared scheme. Case 3: The second compared scheme.

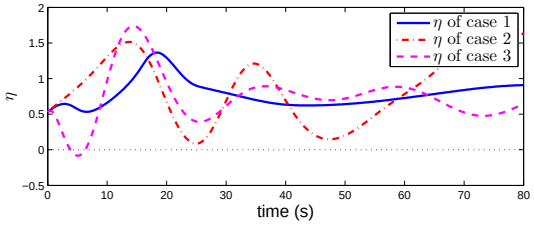

Fig. 2: Variable $\eta(t)$ of three control schemes. Case 1: The proposed scheme. Case 2: The first compared scheme. Case 3: The second compared scheme.

cannot obtain the exact information of its attitude and angular velocity, and therefore the above measured attitude $Q_m(t)$ and the measured angular velocity $w_m(t)$ are employed in the attitude controller.

The values of the control parameters can be seen in Table II. The initial values of the control and system variables are $Q(0) = [0, 1, 0; 0.943, 0, 0.333; 0.333, 0, -0.943]$, $w(0) = \text{col}(-0.045, -0.075, 0.15)$ rad/s, $r_{u,1}(0) = 1$ and $r_{u,2}(0) = 1.5$. The reference angular velocity and reference angular acceleration are $w_d(t) = (0.08 + 0.01\sin(0.2t))n_r$ rad/s and $a_d(t) = 0.002\cos(0.2t)n_r$ rad/s^2 with $n_r = \text{col}(0.9923, 0, 0.1240)$, and the initial value of the reference attitude is $Q_d(0) = [0, 1, 0; -1, 0, 0; 0, 0, 1]$.

To show the performance of the proposed scheme, two control schemes are introduced as the compared schemes. The control scheme similar to [44] is employed as the first compared scheme, and the according virtual controller is

$$w_c = -k_{c,1}(B_R e_{Q,C} + C_R e_{Q,B}), \tag{65}$$

where $B_R = 1 - k_{c,2}\ln(\frac{\eta}{1+\cos\theta_f})$, $C_R = \frac{1}{2}\text{Tr}(A_c(E_3 - Q_{er}))$, $e_{R,B} = -\frac{k_{c,2}}{\eta}S(Q^T v_f)v_{b,1}$, $e_{R,C} = \frac{1}{2}\text{Pa}(A_c Q_{er})$, the operator $\text{Pa}(\cdot)$ is defined in Notations, and $A_c = \text{diag}(a_{c,1}, a_{c,2}, a_{c,3})$ with $a_{c,i} > 0$ for $i = 1, 2, 3$ and $a_{c,i} \neq a_{c,j}$ for any $i \neq j$. The control input (57) and the according adaptive laws (58a)-(58b) are still employed in the above compared control scheme. Note that the repulsive term $B_R(Q_{er}(t))$ on the attitude constraint (4) and the associated vector $e_{R,B}(Q_{er}(t))$ are contained in the virtual controller (65). The function of the term $B_R(Q_{er}(t))$ and the vector $e_{R,B}(Q_{er}(t))$ is to make the spacecraft attitude keep away

from the attitude forbidden zone [44]. The design procedure on the above virtual controller w_c (65) and the rigorous proof of satisfying the attitude constraint can be seen in [44].

Besides, the prescribed performance attitude control scheme similar to [60] is also introduced as the second compared control scheme, and the associated virtual controller is

$$w_c = \bar{w}_d + B_Q^{-1}(B_e e_\zeta - B_\zeta^{-1}\zeta), \tag{66}$$

where $e_\zeta = \mathrm{col}(e_{\zeta,1}, e_{\zeta,2}, e_{\zeta,3}) = \frac{1}{2\sqrt{1+\mathrm{Tr}(Q_{er})}}\mathrm{Pa}(Q_{er}) \in \mathbb{R}^3$, $B_Q = \frac{1}{2\sqrt{1+\mathrm{Tr}(Q_{er})}}(\mathrm{Tr}(Q_{er})E_3 - Q_{er}^T + 2e_\zeta e_\zeta^T) \in \mathbb{R}^{3\times 3}$, $\zeta = (\mathcal{T}_{\zeta,1}(e_{\zeta,1}/\rho_{\zeta,1}), \mathcal{T}_{\zeta,2}(e_{\zeta,2}/\rho_{\zeta,2}), \mathcal{T}_{\zeta,3}(e_{\zeta,3}/\rho_{\zeta,3})) \in \mathbb{R}^3$, $B_\zeta = \mathrm{diag}(\frac{d\mathcal{T}_{\zeta,1}}{d(e_{\zeta,1}/\rho_{\zeta,1})\rho_{\zeta,1}}, \frac{d\mathcal{T}_{\zeta,2}}{d(e_{\zeta,2}/\rho_{\zeta,2})\rho_{\zeta,2}}, \frac{d\mathcal{T}_{\zeta,3}}{d(e_{\zeta,3}/\rho_{\zeta,3})\rho_{\zeta,3}}) \in \mathbb{R}^{3\times 3}$, $B_e = \mathrm{diag}(\frac{\dot{\rho}_{\xi,1}}{\rho_{\xi,1}}, \frac{\dot{\rho}_{\xi,2}}{\rho_{\xi,2}}, \frac{\dot{\rho}_{\xi,3}}{\rho_{\xi,3}})$, with $\mathcal{T}_{\zeta,i}(\cdot)$ and $\rho_{\zeta,i}(t)$, $i = 1, 2, 3$, being the prescribed performance transformation functions and the decaying functions respectively [60]. The control input (57) and the according adaptive laws (58a)-(58b) are still used in the above compared control scheme. It is worth mentioning that the above control schemes similar to [60] can possess the prescribed control performance.

The simulation results of three control schemes can be seen in Figs. 1-2, where the green dotted lines in Figs. 1(b)-(d) are the decaying functions $\rho_1(t)$, $\rho_2(t)$ and $\rho_3(t)$, respectively. The regions surrounded by the green dotted line and the x-y axes are the according appointed-time performance constraints. The functions $\varphi_1(t)$, $\varphi_2(t)$ and $\varphi_3(t)$ can meet the appointed-time control performance, if they are located in the above regions.

First, it can be seen in Figs. 1(e)-(h) that within 80 s, $w(t)$, $r_{u,1}(t)$, $r_{u,2}(t)$ and $\tau(t)$ of three control schemes are all bounded, $r_{u,1}(t) \geq 0$ and $r_{u,2}(t) \geq 0$. However, it can be seen in Figs. 1(a)-(d) and Fig. 2 that the attitude tracking performance of the proposed scheme differs from that of these two compared schemes.

For the proposed scheme, on one hand, the attitude tracking error $Q_{er}(t)$ in Fig. 1(a) converges into the small neighborhood of the equilibrium E_3 within 50 s and remains in this neighborhood after 50 s. This is because the appointed-time performance requirements (28), (30) and (31) are considered in the proposed scheme. In fact, in Fig. 1(b), different from the first compared control scheme (65), the error function $\varphi_1(t)$ of the proposed control scheme always satisfies the constraint (28) within 50 s, meaning that the error function $\varphi_1(t)$ of the proposed control scheme can converge into the interval $[0, 0.3)$ within 25 s and can remain in this interval after 25 s. Besides, in Figs. 1(c)-(d), different from the first compared control scheme (65) and the second compared control scheme (66), the error function $\varphi_2(t)$ of the proposed control scheme satisfies the constraint (30) when $25\text{ s} \leq t \leq 35$ s, and the error function $\varphi_3(t)$ of the proposed control scheme also satisfies the constraint (31) when $t \geq 35$ s. Based upon Theorem 1, this means that the attitude tracking error $Q_{er}(t)$ can remain in the set Θ_R (32) after 50 s. On the other hand, in Fig. 2, the proposed control scheme can meet the attitude constraint (4) within 80 s. The reason is that by virtue of the projection function (16)-(17), the designed control scheme can meet the attitude constraint (4) at all the time.

However, it can be seen in Figs. 1(a)-(d) and Fig. 2 that the compared control schemes cannot meet the attitude constraint and the appointed-time control performance simultaneously. On one hand, for the first compared control scheme (65), it is shown in Fig. 2 that the associated spacecraft attitude can meet the attitude constraint (4) within 80 s. However, compared with the proposed scheme, the corresponding attitude tracking error $Q_{er}(t)$ in Fig. 1(a) does not possess the small convergence time and the small steady-state error. This is because the appointed-time performance constraints (28), (30) and (31) are not considered in the first compared scheme, and therefore in Figs. 1(b)-(d), the according error functions $\varphi_1(t)$, $\varphi_2(t)$ and $\varphi_3(t)$ violate the constraints (28), (30) and (31). On the other hand, for the second compared control scheme (66), it is shown in Fig. 1(a) that the according spacecraft attitude can fast track the reference attitude. However in Fig. 2, the corresponding spacecraft attitude cannot meet the attitude constraint (4). This reason is that the second compared control scheme does not consider the attitude constraint (4). In all, it is concluded from Figs. 1-2 that, distinct with the above compared control schemes, the proposed control scheme can meet the attitude constraint and the appointed-time control performance simultaneously, even in the presence of the parameter uncertainties, the external disturbances and the measurement noises.

V. Conclusions

This paper studies the constrained attitude tracking control of the spacecraft with the appointed-time control performance. A novel projection function is developed to map the boresight vector to the according reduced dimensional vector, and the attitude constraint will be satisfied if the reduced dimensional vector is uniformly bounded. Then a set of vector-based error functions, the appointed-time performance constraints, and the corresponding adaptive controller are carefully constructed. Based on the derived $SO(3)$-based attitude control scheme, the spacecraft attitude can possess the appointed-time control performance and avoid the attitude forbidden zone simultaneously, and is robust to the parameter uncertainties and the external disturbances. In the future, inspired by [40]-[45], the authors intend to investigate the prescribed performance attitude synchronization control of multiple spacecraft with the attitude constraints.

Appendix A
Proof of Lemma 6

First, it is obtained from $\varphi_1 < \rho_{\infty,1}$ and Remark 3 that the Eqs. (33)-(34) and (36) hold. Besides, it is obtained from (23b), (24b) and $v_{r,2}^T v_{r,1} = 0$ that

$$\begin{aligned} v_{r,2}^T v_{r,d,2} &= v_{r,2}^T(E_3 - v_{r,1}v_{r,1}^T)v_{r,d,2} \\ &= \|\tilde{v}_{r,d,3}\| v_{r,2}^T \bar{v}_{r,d,3}. \end{aligned} \tag{67}$$

Therefore, based upon $\varphi_3 = 1 - v_{r,2}^T\bar{v}_{r,d,3} < \rho_{\infty,3} < 1$, (36) and (67), it is further obtained that

$$\begin{aligned} 1 - v_{r,2}^T v_{r,d,2} &= 1 - \|\tilde{v}_{r,d,3}\| v_{r,2}^T \bar{v}_{r,d,3} \\ &< 1 - (1-\rho_{\infty,1})(1-\rho_{\infty,3}). \end{aligned} \tag{68}$$

Then denote $A_R \triangleq v_{b,1}v_{b,1}^T + v_{b,2}v_{b,2}^T$. Based upon (33), (68) and the relations $v_{r,i} = Qv_{b,i}$ and $v_{r,d,i} = Q_d v_{b,i}$, if $\varphi_1 < \rho_{\infty,1}$ and $\varphi_3 < \rho_{\infty,3}$, then $\mathrm{Tr}(A_R - A_R Q_{er})$ is scaled as

$$\begin{aligned}\mathrm{Tr}(A_R - A_R Q_{er}) &= 2 - v_{r,d,1}^T v_{r,1} - v_{r,d,2}^T v_{r,2} \\ &< 1 - (1-\rho_{\infty,1})(1-\rho_{\infty,3}) + \rho_{\infty,1} \\ &< 2\rho_{\infty,1} + \rho_{\infty,3}.\end{aligned} \tag{69}$$

Moreover, since the eigenvalues of A_R are 1, 1 and 0, it is further obtained from Lemma 1 and (69) that

$$\begin{aligned}\mathrm{Tr}(E_3 - E_3 Q_{er}) &\le 2\mathrm{Tr}(A_R - A_R Q_{er}) \\ &< 4\rho_{\infty,1} + 2\rho_{\infty,3},\end{aligned} \tag{70}$$

if $\varphi_1 < \rho_{\infty,1}$ and $\varphi_3 < \rho_{\infty,3}$.

REFERENCES

[1] S. Nicosia, and P. Tomei, "Nonlinear observer and output feedback attitude control of spacecraft," *IEEE Trans. Aerosp. Electron. Syst.*, vol. 28, no. 4, pp. 970-977, Oct. 1992.

[2] S. N. Singh, and A. Iyer, "Nonlinear decoupling sliding mode control and attitude control of spacecraft," *IEEE Trans. Aerosp. Electron. Syst.*, vol. 25, no. 5, pp. 621-633, Sep. 1989.

[3] J. L. Crassidis, S. R. Vadali, and F. L. Markley, "Optimal variable-structure control tracking of spacecraft maneuvers," *J. Guid. Control Dyn.*, vol. 23, no. 3, pp. 564-566, May 2000.

[4] J. A, Zhao, Y. L. Fu, J. M. Ma, J. Fu, Q. Chao, and Y. Wang, "Review of cylinder block/valve plate interface in axial piston pumps: theoretical models, experimental investigations, and optimal design," *Chin. J. Aeronaut.*, vol. 34, no. 1, pp. 111-134, Jan. 2021.

[5] L., Zhao, J. P. Yu, and P. Shi, "Command filtered backstepping-based attitude containment control for spacecraft formation," *IEEE Trans. Syst. Man Cybern. -Syst.*, vol. 51, no. 2, pp. 1278-1287, Feb. 2021.

[6] F. Bullo, and R. M. Murray, "Tracking for fully actuated mechanical systems: a geometric framework," *Automatica*, vol. 35, no. 1, pp. 17-34, Jan. 1999.

[7] F. Bayat, and M. Javaheri, "Two-layer terminal sliding mode attitude control of satellites equipped with reaction wheels," *Asian J. Control*, vol. 22, no. 1, pp. 388-397, Jan. 2020.

[8] Y. Wang, T. S. Shen, C. S. Tan, J. Fu, and S. R. Guo, "Research status, critical technologies, and development trends of hydraulic pressure pulsation attenuator," *Chin. J. Mech. Eng.*, vol. 34, no. 1, pp. 1-17, Jan. 2021.

[9] B. Xiao, L. Cao, and D. C. Ran, "Attitude exponential stabilization control of rigid bodies via disturbance observer," *IEEE Trans. Syst. Man Cybern. -Syst.*, vol. 51, no. 5, pp. 2751-2759, May 2021.

[10] A. M. Zou, and K. D. Kumar, "Finite-time attitude control for rigid spacecraft subject to actuator saturation," *Nonlinear Dyn.*, vol. 96, no. 2, pp. 1017-1035, Apr. 2019.

[11] Z. J. Liu, J. K. Liu, and L. J. Wang, "Disturbance observer based attitude control for flexible spacecraft with input magnitude and rate constraints," *Aerosp. Sci. Technol.*, vol. 72, pp. 486-492, Jan. 2018.

[12] M. Tafazoli, "A study of on-orbit spacecraft failures," *Acta Astronaut.*, vol. 64, no. 2-3, pp. 195-205, Jan. 2009.

[13] Z. J. Liu, Z. J. Han, Z. J. Zhao, and W. He, "Modeling and adaptive control for a spatial flexible spacecraft with unknown actuator failures," *Sci. China-Inf. Sci.*, vol. 64, no. 5, pp. 1-16, May 2021.

[14] L. H. Kong, W. He, C. G. Yang, and C. Y. Sun, "Robust neurooptimal control for a robot via adaptive dynamic programming," *IEEE Trans. Neural Netw. Learn. Syst.*, vol. 32, no. 6, pp. 2584-2594, Jun. 2021.

[15] B. Xiao, Q. L. Hu, and Y. M. Zhang, "Adaptive sliding mode fault tolerant attitude tracking control for flexible spacecraft under actuator saturation," *IEEE Trans. Control Syst. Technol.*, vol. 20, no. 6, pp. 1605-1612, Nov. 2012.

[16] S. H. Ding, and S. H. Li, "Stabilization of the attitude of a rigid spacecraft with external disturbances using finite-time control techniques," *Aerosp. Sci. Technol.*, vol. 13, no. 4-5, pp. 256-265, Jun. 2009.

[17] K. S. Kim, and Y. D. Kim, "Robust backstepping control for slew maneuver using nonlinear tracking function," *IEEE Trans. Control Syst. Technol.*, vol. 11, no. 6, pp. 822-829, Nov. 2003.

[18] L. H. Kong, W. He, C. G. Yang, Z. J. Li, and C. Y. Sun, "Adaptive fuzzy control for coordinated multiple robots with constraint using impedance learning," *IEEE Trans. Cybern.*, vol. 49, no. 8, pp. 3052-3063, Aug. 2019.

[19] W. He, C. Q. Xue, X. B. Yu, Z. J. Li, and C. G. Yang, "Admittance-based controller design for physical human-robot interaction in the constrained task space," *IEEE Trans. Autom. Sci. Eng.*, vol. 17, no. 4, pp. 1937-1949, Oct. 2020.

[20] Y. M. Park, M. J. Tahk, J. Y. Park, "Optimal stabilization of Takagi-Sugeno fuzzy systems with application to spacecraft control," *J. Guid. Control Dyn.*, vol. 24, no. 4, pp. 767-777, Jul. 2001.

[21] L. H. Kong, W. He, Y. T. Dong, L. Cheng, C. G. Yang, and Z. J. Li, "Asymmetric bounded neural control for an uncertain robot by state feedback and output feedback," *IEEE Trans. Syst. Man Cybern. -Syst.*, vol. 51, no. 3, pp. 1735-1746, Mar. 2021.

[22] Y. Liu, B. X. Jiang, J. Q. Lu, J. D. Cao, and G. P, Lu, "Event-triggered sliding mode control for attitude stabilization of a rigid spacecraft," *IEEE Trans. Syst. Man Cybern. -Syst.*, vol. 50, no. 9, pp. 3290-3299, Sep. 2020.

[23] F. Bayat, "Model predictive sliding control for finite-time three-axis spacecraft attitude tracking," *IEEE Trans. Ind. Electron.*, vol. 66, no. 10, pp. 7986-7996, Oct. 2019.

[24] Y. Han, J. D. Biggs, and N. G. Cui, "Adaptive fault-tolerant control of spacecraft attitude dynamics with actuator failures," *J. Guid. Control Dyn.*, vol. 38, no. 10, pp. 2033-2042, Oct. 2015.

[25] A. M. Zou, and K. D. Kumar, "Adaptive fuzzy fault-tolerant attitude control of spacecraft," *Control Eng. Practice*, vol. 19, no. 1, pp. 10-21, Jan. 2011.

[26] L. Sun, "Constrained adaptive fault-tolerant attitude tracking control of rigid spacecraft," *Adv. Space Res.*, vol. 63, no. 7, pp. 2229-2238, Apr. 2019.

[27] B. Y. Huo, Y. Q. Xia, K. F. Lu, and M. Y. Fu, "Adaptive fuzzy finite-time fault-tolerant attitude control of rigid spacecraft," *J. Franklin Inst.*, vol. 352, no. 10, pp. 4225-4246, Oct. 2015.

[28] L. Sun, "Adaptive fault-tolerant constrained control of cooperative spacecraft rendezvous and docking," *IEEE Trans. Ind. Electron.*, vol. 67, no. 4, pp. 3107-3115, Apr. 2020.

[29] A. Sanyal, A. Fosbury, N. Chaturvedi, and D. S. Bernstein, "Inertia-free spacecraft attitude tracking with disturbance rejection and almost global stabilization," *J. Guid. Control Dyn.*, vol. 32, no. 4, pp. 1167-1178, Jul. 2009.

[30] C. G. Mayhew, and A. R. Teel, "Synergistic hybrid feedback for global rigid-body attitude tracking on $SO(3)$," *IEEE Trans. Autom. Control*, vol. 58, no. 11, pp. 2730-2742, Nov. 2013.

[31] S. Berkane, and A. Tayebi, "Construction of synergistic potential functions on $SO(3)$ with application to velocity-free hybrid attitude stabilization," *IEEE Trans. Autom. Control*, vol. 62, no. 1, pp. 495-501, Jan. 2017.

[32] A. Sarlette, R. Sepulchre, and N. E Leonard, "Autonomous rigid body attitude synchronization," *Automatica*, vol. 45, no. 2, pp. 572-577, Feb. 2009.

[33] J. Thunberg, W. J. Song, E. Montijano, Y. G. Hong, and X. M. Hu, "Distributed attitude synchronization control of multi-agent systems with switching topologies," *Automatica*, vol. 50, no. 3, pp. 832-840, Mar. 2014.

[34] J. R. Forbes, "Passivity-based attitude control on the special orthogonal group of rigid-body rotations," *J. Guid. Control Dyn.*, vol. 36, no. 6, pp. 1596-1605, Nov. 2013.

[35] Y. Zou, and Z. Y. Meng, "Velocity-free leader-follower cooperative attitude tracking of multiple rigid bodies on $SO(3)$," *IEEE Trans. Cybern.*, vol. 49, no. 12, pp. 4078-4089, Dec. 2019.

[36] H. C. Kjellberg, and E. G. Lightsey, "Discretized constrained attitude pathfinding and control for satellites," *J. Guid. Control Dyn.*, vol. 36, no. 5, pp. 1301-1309, Sep. 2013.

[37] R. Dai, and C. C. Sun, "Path planning of spatial rigid motion with constrained attitude," *J. Guid. Control Dyn.*, vol. 38, no. 8, pp. 1356-1365, Aug. 2015.

[38] C. Q. Wu, R. Xu, S. Y. Zhu, and P. Y. Cui, "Time-optimal spacecraft attitude maneuver path planning under boundary and pointing constraints," *Acta Astronaut.*, vol. 137, pp. 128-137, Aug. 2017.

[39] Y. S. Kim, and M. Mesbahi, "Quadratically constrained attitude control via semidefinite programming," *IEEE Trans. Autom. Control*, vol. 49, no. 5, pp. 731-735, May 2004.

[40] U. Lee, and M. Mesbahi, "Feedback control for spacecraft reorientation under attitude constraints via convex potentials," *IEEE Trans. Aerosp. Electron. Syst.*, vol. 50, no. 4, pp. 2578-2592, Oct. 2014.

[41] Q. Shen, C. F. Yue, C. H. Goh, B. L. Wu, D. W. Wang, "Rigid-body attitude stabilization with attitude and angular rate constraints," *Automatica*, vol. 90, pp. 157-163, Apr. 2018.

[42] Q. L. Hu, Y. Y. Liu, H. Y. Dong, and Y. M. Zhang, "Saturated attitude control for rigid spacecraft under attitude constraints," *J. Guid. Control Dyn.*, vol. 43, no. 4, pp. 790-805, Apr. 2020.

[43] M. M. Nicotra, D. Liao-McPherson, L. Burlion, I. V. Kolmanovsky, "Spacecraft attitude control with nonconvex constraints: an explicit reference governor approach," *IEEE Trans. Autom. Control*, vol. 65, no. 8, pp. 3677-3684, Aug. 2020.

[44] S. Kulumani, and T. Y. Lee, "Constrained geometric attitude control on $SO(3)$," *Int. J. Control Autom. Syst.*, vol. 15, no. 6, pp. 2796-2809, Dec. 2017.

[45] T., Chen, and J. J. Shan, "Continuous constrained attitude regulation of multiple spacecraft on $SO(3)$," *Aerosp. Sci. Technol.*, vol. 99, 105769, Apr. 2020.

[46] C. S. Wei, J. J. Luo, H. H. Dai, and G. R. Duan, "Learning-based adaptive attitude control of spacecraft formation with guaranteed prescribed performance," *IEEE Trans. Cybern.*, vol. 49, no. 11, pp. 4004-4016, Nov. 2019.

[47] Y. Huang, and Y. M. Jia, "Adaptive fixed-time six-DOF tracking control for noncooperative spacecraft fly-around mission," *IEEE Trans. Control Syst. Technol.*, vol. 27, no. 4, pp. 1796-1804, Jul. 2018.

[48] C. P. Bechlioulis, G. A. Rovithakis, "Robust adaptive control of feedback linearizable MIMO nonlinear systems with prescribed performance," *IEEE Trans. Autom. Control*, vol. 53, no. 9, pp. 2090-2099, Oct. 2008.

[49] C. P. Bechlioulis, and G. A. Rovithakis, "Robust partial-state feedback prescribed performance control of cascade systems with unknown nonlinearities," *IEEE Trans. Autom. Control*, vol. 56, no. 9, pp. 2224-2230, Sep. 2011.

[50] S. B. Wang, J. Na, and X. M. Ren, "RISE-based asymptotic prescribed performance tracking control of nonlinear servo mechanisms," *IEEE Trans. Syst. Man Cybern. -Syst.*, vol. 48, no. 12, pp. 2359-2370, Dec. 2017.

[51] J. J. Luo, Z. Y. Yin, C. S. Wei, and J. P. Yuan, "Low-complexity prescribed performance control for spacecraft attitude stabilization and tracking," *Aerosp. Sci. Technol.*, vol. 74, pp. 173-183, Mar. 2018.

[52] Y. B. Hu, Y. H. Geng, B. L. Wu, and D. W. Wang, "Model-free prescribed performance control for spacecraft attitude tracking," *IEEE Trans. Control Syst. Technol.*, vol. 29, no. 1, pp. 165-179, Mar. 2021.

[53] C. F. Yue, F. Wang, X. B. Cao, Q. Shen, and X. Q. Chen, "Robust fault-tolerant attitude tracking with guaranteed prescribed performance," *J. Franklin Inst.*, vol. 357, no. 1, pp. 229-253, Jan. 2020.

[54] Q. L. Hu, X. D. Shao, and L. Guo, "Adaptive fault-tolerant attitude tracking control of spacecraft with prescribed performance," *IEEE-ASME Trans. Mechatron.*, vol. 23, no. 1, pp. 331-341, Feb. 2018.

[55] X. D. Shao, Q. L. Hu, Y. Shi, and B. Y. Jiang, "Fault-tolerant prescribed performance attitude tracking control for spacecraft under input saturation," *IEEE Trans. Control Syst. Technol.*, vol. 28, no. 2, pp. 574-582, Mar. 2020.

[56] X. W. Huang, J. D. Biggs, and G. R. Duan, "Post-capture attitude control with prescribed performance," *Aerosp. Sci. Technol.*, vol. 96, 105572, Jan. 2020.

[57] C. Zhang, G. F. Ma, Y. C. Sun, and C. J. Li, "Prescribed performance adaptive attitude tracking control for flexible spacecraft with active vibration suppression," *Nonlinear Dyn.*, vol. 96, no. 3, pp. 1909-1926, May 2019.

[58] M. M. Liu, X. D. Shao, and G. F. Ma, "Appointed-time fault-tolerant attitude tracking control of spacecraft with double-level guaranteed performance bounds," *Aerosp. Sci. Technol.*, vol. 92, pp. 337-346, Sep. 2019.

[59] X. H. Peng, Z. Y. Geng, and J. Y. Sun, "The specified finite-time distributed observers-based velocity-free attitude synchronization for rigid bodies on $SO(3)$," *IEEE Trans. Syst. Man Cybern. -Syst.*, vol. 50, no. 4, pp. 1610-1621, Apr. 2020.

[60] Z. G. Zhou, Y. A. Zhang, X. N. Shi, and D. Zhou, "Robust attitude tracking for rigid spacecraft with prescribed transient performance," *Int. J. Control*, vol. 90, no. 11, pp. 2471-2479, Nov. 2017.

[61] X. H. Lu, Y. M. Jia, Y. L. Fu, and F. Matsuno, "Projection function design on attitude constraint of the spacecraft", *Preprints in HAL*, 2021. https://hal.archives-ouvertes.fr/hal-02882922/.

[62] F. Zhang, and G. R. Duan, "Robust adaptive integrated translation and rotation control of a rigid spacecraft with control saturation and actuator misalignment," *Acta Astronaut.*, vol. 86, pp. 167-187, May 2013.

[63] P. Baldi, P. Castaldi, N. Mimmo, and S. Simani, "A new aerodynamic decoupled frequential FDIR methodology for satellite actuator faults," *Int. J. Adapt. Control Signal Process.*, vol. 28, no. 9, pp. 812-832, Sep. 2014.

[64] J. R. Wertz, *Spacecraft Attitude Determination and Control*. Dordrecht, Netherlands: Kluwer Academic Publishers, 1978.

[65] W. J. Larson, and J. R. Wertz, *Space Mission Analysis and Design*. El Segundo, CA: Microcosm Press and Kluwer Academic Publishers, 1999.